Nardilysin is Required for maintaining Pancreatic β-Cell Function

Kiyoto Nishi,[1] Yuichi Sato,[2] Mikiko Ohno,[1] Yoshinori Hiraoka,[1,4] Sayaka Saijo,[1] Jiro Sakamoto,[1] Po-Min Chen,[1] Yusuke Morita,[1] Shintaro Matsuda,[1] Kanako Iwasaki,[2] Kazu Sugizaki,[2] Norio Harada,[2] Yoshiko Mukumoto,[5] Hiroshi Kiyonari,[5,6] Kenichiro Furuyama,[3] Yoshiya Kawaguchi,[3,7] Shinji Uemoto,[3] Toru Kita,[8] Nobuya Inagaki,[2] Takeshi Kimura[1] and Eiichiro Nishi[1*]

[1]Department of Cardiovascular Medicine

[2]Department of Diabetes, Endocrinology and Nutrition

[3]Department of Surgery

Graduate School of Medicine, Kyoto University, 54 Shogoin-Kawahara-cho, Sakyo-ku, Kyoto 606-8507, Japan

[4]Division of Clinical Pharmacy, Faculty of Pharmaceutical Sciences, Kobe Gakuin University, 1-1-3 Minatojima, Chuo-ku, Kobe 650-8586, Japan

[5]Genetic Engineering Team

[6]Animal Resource Development Unit

RIKEN Center for Life Science Technologies, 2-2-3 Minatojima Minami, Chuo-ku, Kobe 650-0047, Japan

[7]Department of Clinical Application, Center for iPS Cell Research and Application, Kyoto University, 53 Shogoin-Kawahara-cho, Sakyo-ku, Kyoto 606-8507, Japan

Diabetes Publish Ahead of Print, published online July 6, 2016

[8]Kobe City Medical Center General Hospital, 4-6 Minatojima-nakamachi, Chuo-ku, Kobe 650-0046, Japan

*Corresponding author

Correspondence should be addressed to E.N. (nishi@kuhp.kyoto-u.ac.jp).

SUMMARY

Type 2 diabetes (T2D) is associated with pancreatic β-cell dysfunction, manifested by reduced glucose-stimulated insulin secretion (GSIS). Several transcription factors enriched in β-cells, such as MafA, control β-cell function by organizing genes involved in GSIS. Here, we demonstrate that nardilysin (N-arginine dibasic convertase; *Nrd1* and NRDc) critically regulates β-cell function through MafA. *Nrd1*$^{-/-}$ mice showed glucose intolerance and severely decreased GSIS. Islets isolated from *Nrd1*$^{-/-}$ mice exhibited reduced insulin content and impaired GSIS *in vitro*. Moreover, β-cell-specific NRDc-deficient (*Nrd1*^{delβ}) mice showed a diabetic phenotype with markedly reduced GSIS. MafA was specifically downregulated in islets from *Nrd1*^{delβ} mice, whereas overexpression of NRDc upregulated MafA and insulin expression in INS 832/13 cells. Chromatin immunoprecipitation assay revealed that NRDc is associated with Islet-1 in the enhancer region of MafA, where NRDc controls the recruitment of Islet-1 and MafA transcription. Our findings demonstrate that NRDc controls β-cell function via regulation of the Islet-1-MafA pathway.

INTRODUCTION

Type 2 diabetes (T2D) is a common metabolic disorder, which afflicts more than 300 million people globally (1). It is characterized by impaired insulin secretion from pancreatic β-cells and insulin resistance of the target tissues, such as liver, adipose tissue and muscles. Although both factors play important roles in the pathogenesis of the disease, β-cell dysfunction, mainly manifested by deteriorated glucose-stimulated insulin secretion (GSIS), appears to be predominant for the transition from simple obesity to T2D (2). The observation that the impaired GSIS in islets from T2D patients cannot be accounted for by reduced insulin content also supports this concept (1). Several biological processes including endoplasmic reticulum stress, inflammation and oxidative stress are suggested to impair GSIS in T2D (3, 4).

The pancreas is composed of an exocrine compartment, consisting of acinar and ductal cells, and an endocrine compartment, consisting of α, β, δ, ε and PP cells. These different types of endocrine cell express and secrete the hormones glucagon, insulin, somatostatin, ghrelin and pancreatic polypeptide, respectively. Sequential expression of pancreatic transcription factors determines the cell fate and pancreatic development. Among them, several transcriptional factors enriched in β-cells, such as Pdx-1, Nkx6.1 and MafA, play essential roles in the maintenance of β-cell identity and function. β-cell-specific ablation of *Pdx-1* results in hyperglycemia with reduced insulin-positive cells and increased glucagon-positive cells (5, 6), whereas conditional *Nkx6.1* inactivation in adult β-cells causes reduced insulin production (7). In contrast to

the earlier expression of Pdx-1 and Nkx6.1 in endocrine progenitor cells, MafA is first produced at E13.5 and only observed in insulin-positive mature β-cells. MafA binds to an insulin promoter, like Pdx-1, and regulates β-cell-selective insulin transcription (8). Consistently, *Mafa*-deficient mice develop diabetes due to impaired GSIS without a defect of islet cell development (9). Moreover, β-cell-specific ablation of pan-endocrine transcription factors like NeuroD1 and Islet-1 demonstrated their critical roles in β-cell maturation and function (10, 11). In particular, postnatal ablation of *Islet-1* in β-cells resulted in impaired GSIS without significantly reducing β-cell mass (11). Collectively, these findings demonstrated that transcription factors involved in the determination of endocrine or β-cell identity also play essential roles in β-cell functions.

Regulatory network of β-cell-enriched transcriptional factors (e.g. Pdx-1, NeuroD1, NKx6.1 and MafA) critically controls GSIS (5-10). These transcriptional factors also connect oxidative stress with impaired GSIS in diabetic mouse models and T2D human (4). Among them, several lines of evidence have suggested that the Islet-1-MafA pathway critically controls GSIS in adults. First, ablation of these genes in β-cells results in impaired GSIS without a severe defect of β-cell development, as described above (9, 11). Second, MafA is a direct target gene of Islet-1 (11, 12). Third, MafA directly regulates several genes critical for GSIS, such as Ins1, Ins2 and Glut2 (also known as Slc2a2).

In the current study, we demonstrate a novel regulatory mechanism of GSIS by nardilysin (N-arginine dibasic convertase; *Nrd1* and NRDc) through the Islet-1-MafA pathway. NRDc is a zinc peptidase of the M16 family, which selectively cleaves

dibasic sites (13, 14). We rediscovered NRDc as a specific receptor for heparin-binding EGF-like growth factor (HB-EGF) (15), and our subsequent studies have shown multiple functions of NRDc, which depend on its cellular localization. In the extracellular space, NRDc enhances ectodomain shedding of HB-EGF and other membrane proteins, such as TNF-α, amyloid precursor protein (APP) and neuregulin-1 (16-20) We have also revealed that NRDc in the nucleus works as a transcriptional coregulator through the modulation of NCoR/SMRT corepressor or PGC-1α coactivator function (21, 22). We show here that NRDc-deficient (*Nrd1*$^{-/-}$) mice and pancreatic β-cell-specific NRDc-deficient (*Nrd1*^{delβ}) mice show glucose intolerance and severely impaired glucose-stimulated insulin secretion (GSIS). Islets isolated from *Nrd1*$^{-/-}$ and *Nrd1*^{delβ} mice also show lower insulin production and GSIS than wild-type islets. Notably, NRDc and Islet-1 colocalize in the MafA enhancer, where NRDc regulates the recruitment of Islet-1 and MafA transcription, indicating the essential role of NRDc in GSIS through Islet-1-MafA regulation.

Materials and methods

Animals

Nrd1$^{-/-}$ mice (Accession No. CDB0466K, http://www.clst.riken.jp/arg/mutant%20mice%20list.html) were generated as described previously (19), and backcrossed to the ICR background (>98%). *Nrd1*$^{flox/flox}$ mice (Accession No. CDB1019K, http://www.clst.riken.jp/arg/mutant%20mice%20list.html) were generated by gene targeting in TT2 (23) embryonic stem (ES) cells (http://www.clst.riken.jp/arg/Methods.html). The targeting vector was designed to insert loxP sites upstream and downstream of exon 1 of *Nrd1* (Supplementary Fig. 1A). Successful homologous recombination in TT2-ES cells was confirmed by PCR (Supplementary Fig. 1A) and Southern blotting. Resulting mutant mice were genotyped with tail DNA by PCR(Supplementary Fig. 1B) and crossed with CAG-FLPe transgenic mice for the removal of the neomycin selection cassette surrounded by FRT sites, then backcrossed to the C57BL/6J background (>98%). β-cell-specific NRDc-deficient mice were generated by crossing *Nrd1*$^{floxed/floxed}$ mice with rat insulin II promoter-Cre transgenic mice (RIP-Cre) (24). Male mice were used unless otherwise indicated. All animal experiments were performed according to procedures approved by the Institute of Laboratory Animals, Kyoto University. Mice were maintained on a diet of standard rodent chow in environmentally controlled rooms.

Glucose and insulin tolerance tests

For glucose tolerance tests, mice were fasted for 16 hr and intraperitoneally injected with 2 g/kg BW of D-glucose. For insulin tolerance tests, mice were fasted for 5 hr and intraperitoneally injected with insulin (Humulin R, Eli Lilly). To determine fasting plasma glucagon levels, mice were fasted for 16 hr. To determine pancreatic insulin content and proinsulin/insulin ratio, whole pancreata were homogenized in 4 ml of a 2% HCl/75% ethanol solution. After neutralization, samples were diluted 1:1000 in PBS

before the measurements of insulin and proinsulin. Glucose was measured using a glucometer. Insulin (MS303; Morinaga Institute of Biological Science, Japan) and proinsulin (AKMPI-111; Shibayagi, Japan) were measured by ELISA. Glucagon was measured by EIA (YK090; Yanaihara Institute, Japan).

Cell culture

MIN6 and INS832/13 cells were generous gifts from Dr. Miyazaki and Dr. Newgard, respectively. *Nrd1*$^{-/-}$ MEFs were prepared as described previously (19). MIN6 cells and *Nrd1*$^{-/-}$ MEFs were grown in Dulbecco's Modified Eagle Medium (4.5 g l^{-1} glucose) supplemented with 10% fetal bovine serum (FBS) and antibiotics. INS832/13 cells were cultured as previously described (25). GM6001 (26) was purchased from Calbiochem (CA). For overexpression or gene knockdown of *Nrd1* or *Mafa* in MIN6 and INS832/13, cells were infected with lentiviral vectors expressing *Nrd1*, *Mafa* or BLOCK-iT™ miR RNAi (Life Technologies) targeting *Nrd1* or *Mafa*, respectively.

Islet isolation and insulin secretion assay

The isolation of pancreatic islets and the measurement of insulin release from the islets were performed as previously described (27). The amount of immunoreactive insulin was determined by radioimmunoassay (Aloka Accuflex γ 7000; Hitachi, Japan).

Insulin secretion from INS832/13 cells (25) was determined as previously described with some modifications (28). In brief, cells cultured on 6-well plates were washed with Krebs-Ringer bicarbonate HEPES (KRBH) buffer (140 mM NaCl, 3.6 mM KCl, 0.5 mM $MgSO_4$, 0.5 mM NaH_2PO_4, 1.5 mM $CaCl_2$, 2 mM $NaHCO_3$ and 10 mM

HEPES, pH 7.4) with 0.1% BSA and 2.8 mM glucose, pre-incubated at 37°C for 2 hr in KRBH with 2.8 mM glucose, and then incubated at 37°C for 2 hr in KRBH with 2.8 mM glucose and 15 mM glucose. Insulin was measured by ELISA (MS303; Morinaga Institute of Biological Science, Japan).

Chromatin immunoprecipitation (ChIP) and Re-ChIP assay

Chromatin was prepared from MIN6 cells (29) as previously described (21). ChIP assays were performed using ChIP-IT® Express Chromatin Immunoprecipitation Kits (Active Motif). Antibodies against NRDc (mouse monoclonal antibody #2E6), PDX-1 (sc-14664X, Santa Cruz), Islet-1 (ab20670, abcam), Neuro D1 (sc-1084X, Santa Cruz) or control IgG (Santa Cruz) were used. For the re-ChIP assay, Re-ChIP-IT® Express Magnetic Chromatin Re-Immunoprecipitation Kits (Active Motif) were used according to the manufacturer's protocol. The primers used are listed in Supplementary Table 1.

Luciferase reporter assays

For the luciferase reporter assays, PicaGene Promoter Vector 2 (PGV-P2; Toyo Ink, Japan) with or without the insertion of MafA R3 (-8118 to -7750 relative to the transcriptional start site of *Mafa*) was transiently transfected into MIN6 cells. 48 hours after transfection, luciferase activity was quantified by the Dual-Luciferase Reporter Assay Kit (Promega) according to the manufacturer's protocol. pRL-TK (Promega) was co-transfected with PGV-P2 to control for transfection efficiency.

Statistics

Results are expressed as mean ± SEM. Student's t test was used for comparisons between two groups. ANOVA was used for comparisons among multiple groups, with a Tukey-Kramer post hoc test.

Supplemental information

Supplemental information including Supplemental Experimental Procedures, five figures and one table can be found with this article online at doi:

RESULTS

Nrd1$^{-/-}$ mice and islets exhibit impaired glucose-stimulated insulin secretion (GSIS)

We previously reported that *Nrd1*$^{-/-}$ mice show a lean phenotype, which has been attributed to increased energy expenditure due to enhanced thermogenesis in brown adipose tissue and hyperactivity (21). To address whether NRDc is involved in glucose metabolism, we performed the glucose tolerance test and the insulin tolerance test in *Nrd1*$^{-/-}$ mice. Although the fasting blood glucose and serum insulin levels remained the same as in the wild-type (*Nrd1*$^{+/+}$) mice, *Nrd1*$^{-/-}$ mice showed elevated blood glucose levels at 60 and 120 minutes after glucose challenge (Fig. 1A). Importantly, the serum insulin level at 30 minutes after glucose injection was strikingly low in the mutants (Fig. 1B). At the same time, the insulin tolerance test showed the increased insulin sensitivity of *Nrd1*$^{-/-}$ mice (Fig. 1C). On the basis of these observations, the glucose metabolism of the *Nrd1*$^{-/-}$ mice is characterized by mild glucose intolerance and significantly reduced GSIS, accompanied by insulin hypersensitivity.

Histologically, islets of *Nrd1*$^{-/-}$ mice showed no obvious anomalies in their size and structure; there was a predominance of insulin-positive β–cells in the core, which were surrounded by glucagon-positive α-cells (Fig. 1D). Quantitative analysis confirmed no significant difference in β-cell mass and α-cell/β-cell ratio between *Nrd1*$^{+/+}$ and *Nrd1*$^{-/-}$ mice (Fig. 1E, F). Thus, impaired GSIS in *Nrd1*$^{-/-}$ mice is not due to a gross developmental defect in the pancreas, but disturbed islet function was suspected.

To evaluate islet function directly, we isolated islets from *Nrd1*$^{+/+}$ and *Nrd1*$^{-/-}$ mice and performed *in vitro* GSIS assays. Consistent with the *in vivo* results, *Nrd1*$^{-/-}$ islets showed severely reduced GSIS (Fig. 1G) compared with *Nrd1*$^{+/+}$islets. As KCl-induced insulin secretion was preserved in *Nrd1*$^{-/-}$ islets (Fig. 1G), NRDc may regulate GSIS through the processes before membrane depolarization. Insulin content was modestly but significantly reduced in *Nrd1*$^{-/-}$ islets (Fig. 1H). Since NRDc has endopeptidase activity, we examined pancreatic proinsulin/insulin ratios, but found no significant difference between *Nrd1*$^{+/+}$ and *Nrd1*$^{-/-}$ islets (Fig. 1I).

β-cell-specific NRDc-deficient mice show diabetic phenotype with markedly reduced GSIS

The analysis of isolated islets strongly suggested that NRDc is primarily involved in GSIS. To confirm the β-cell-specific role of NRDc, we generated *Nrd1*$^{flox/flox}$ mice by inserting two loxP sites around exon 1 of the mouse *Nrd1* gene (Supplementary Fig. 1A, B) and crossed them with rat insulin II promoter-Cre transgenic mice (RIP-Cre) (24) to produce β-cell-specific NRDc-deficient (*Nrd1*^{delβ}) mice. *Nrd1*^{delβ} mice were born at the expected Mendelian frequency and showed no overt phenotypes including the body weight (Supplementary Fig. 1C). We confirmed the specific decrease of the *Nrd1* mRNA level in pancreatic islets, but not in other organs, including hypothalamus, heart, white adipose tissue, liver and skeletal muscle (Supplementary Fig. 1D). As glucose intolerance and decreased GSIS of RIP-Cre mice has been reported (30), we set two controls, *Nrd1*$^{flox/flox}$ mice and RIP-Cre (*Nrd1*$^{wt/wt}$; RIP-Cre) mice, for the comparison

with *Nrd1*^{delβ} mice. While the global knockout mice showed normal fasting blood glucose (Fig. 1A), *Nrd1*^{delβ} mice demonstrated markedly elevated fasting blood glucose compared with both control mice (Fig. 2A). In glucose tolerance tests, RIP-cre mice showed glucose intolerance and reduced insulin secretion, as previously reported (30), whereas *Nrd1*^{delβ} mice displayed more severe glucose intolerance and more reduced insulin secretion compared with RIP-Cre and *Nrd1*$^{flox/flox}$ mice (Fig. 2B, C). Insulin sensitivity was similar between *Nrd1*$^{flox/flox}$, RIP-Cre and *Nrd1*^{delβ} mice (Supplementary Fig. 1E, F). These results indicated that the β-cell-specific NRDc depletion is sufficient to cause glucose intolerance and impaired GSIS.

Being in sharp contrast to the normal appearance of *Nrd1*$^{-/-}$ islets, islets in *Nrd1*^{delβ} mice showed an impaired structure (Fig. 2D). Glucagon-positive α-cells increased in number with their locations not restricted to the periphery of the islet but intermingled with β-cells at the core. When quantified, α-cell/β-cell ratio was significantly increased in *Nrd1*^{delβ} islets (Fig. 2E). In agreement with these results, fasting plasma glucagon and the mRNA level of islet *Gcg* in *Nrd1*^{delβ} mice were significantly higher than those of control mice (Fig. 2F, G). β-cell mass in *Nrd1*^{delβ} mice was significantly smaller than that in *Nrd1*$^{flox/flox}$ mice and tended to be smaller, though without a statistically significant difference, than RIP-Cre control mice (Fig. 2H). The ratio of large islets was significantly decreased, while that of small islets was increased in *Nrd1*^{delβ} mice compared with either *Nrd1*$^{flox/flox}$ mice or RIP-Cre mice (Fig. 2I).

We also performed a lineage tracing study of insulin-expressing cells in *Nrd1*^{delβ} mice. By crossing *Nrd1*$^{floxed/floxed}$ mice with RIP-Cre and R26ECFP mice (31),

we generated *Nrd1*$^{floxed/floxed}$*;RIP-Cre;R26ECFP* mice, in which the simultaneous deletion of *nrd1* and expression of ECFP occurred specifically in β-cells, and compared them with control *Nrd1*$^{wt/wt}$*;RIP-Cre;R26ECFP* mice (Supplementary Fig. 2A). As shown in Supplementary Fig. 2B and 2C, several ECFP-positive cells lost insulin staining in *Nrd1*$^{floxed/floxed}$*;RIP-Cre;R26ECFP* mice. Furthermore, a small subset of glucagon-positive cells was clearly labelled with ECFP in *Nrd1*$^{floxed/floxed}$*;RIP-Cre;R26ECFP* islets (Supplementary Fig. 2D, E). When quantified, glucagon and ECFP double-positive cells were observed in 3.28% (n=853) of the total glucagon-positive cells in *Nrd1*$^{floxed/floxed}$*;RIP-Cre;R26ECFP* islets, while 0.85% (n=233) in control islets. In addition, genes transiently expressed in endocrine progenitors (e.g. *Sox9*, *Ngn3* and *Mafb*) and *Aldh1a3*, recently reported as a marker of β-cell dedifferentiation , were significantly or tended to be upregulated in *Nrd1*^{delβ} islets (Supplementary Fig. 3A-C). These results suggested that some β-cells may lose their identity and a subset of these β-cells may be converted to glucagon-positive α-like cells in *Nrd1*^{delβ} islets.

MafA is specifically downregulated in islets isolated from *Nrd1*^{delβ} mice

Consistent with the results of the *in vivo* glucose tolerance test, islets isolated from *Nrd1*^{delβ} mice showed markedly reduced GSIS. Compared with islets isolated from *Nrd1*$^{flox/flox}$ and RIP-Cre control mice, both low- (2.8 mM) and high-glucose-stimulated (25 mM) insulin secretion (Fig. 3A) was significantly reduced in *Nrd1*^{delβ} islets. Furthermore, the insulin content of the freshly isolated islets (Fig. 3B) was significantly lower in *Nrd1*^{delβ} mice. To obtain mechanistic insights that explain the reduced insulin

content and impaired GSIS of the *Nrd1*^{delβ} islets, we examined the mRNA levels of genes involved in GSIS and found that *Glut2, Pcx, Ins1, Ins2,* and *Pcsk1* are significantly decreased in *Nrd1*^{delβ} islets compared with those in RIP-cre islets (Fig. 3C). Reduction of *Glut2, Pcx Ins1 and Ins2* levels in *Nrd1*^{delβ} islets was also confirmed when compared with *Nrd1*$^{flox/flox}$ islets. However, *Pcsk1* was increased in *Nrd1*^{delβ} islets compared with that in *Nrd1*$^{flox/flox}$ islets, since it was markedly increased in RIP-cre islets (Supplementary Fig. 4A). We next investigated the expression of transcription factors in β-cells that potentially regulate *Glut2, Pcx, Ins1+2* and *Pcsk1*. Intriguingly, *Mafa* was specifically downregulated in islets from *Nrd1*^{delβ} mice, whereas the expression of *Pdx1* and others including *NKx6.1*, *NeuroD1* and *Islet-1* was not significantly changed (Fig. 3D and Supplementary Fig. 4B). Histological findings confirmed that the reduced protein expression of GLUT2, MafA and insulin in *Nrd1*^{delβ} islets (Fig. 3E, F). These results suggested that NRDc in β-cells acts upstream of MafA.

NRDc regulates insulin production through MafA

Our loss-of-function experiments using *Nrd1*^{delβ} mice/islets revealed that NRDc is essential for proper islet function, especially for GSIS, via maintaining the expression of *Mafa* and its downstream genes such as *Ins1*, *Ins2*, *Glut2* and *Pcsk1*. At the same time, islet structure was impaired in *Nrd1*^{delβ} mice. Considering a previous report describing that abrogated structure itself disturbs islet function (32), we were prompted to perform loss-of-function or gain-of-function experiments in a β-cell line to confirm the cell autonomous role of NRDc. INS 832/13 cells are an INS-1-derived rat β-cell line that are

strongly responsive to glucose in terms of insulin secretion (25). Similar to *Nrd1*$^{del\beta}$ islets, *Nrd1*-knocked down INS 832/13 (Fig. 4A) showed decreased insulin secretion (Fig. 4B), insulin content (Fig. 4C) and mRNA levels of genes involved in insulin secretion (Fig. 4D). On the other hand, INS 832/13 cells, in which NRDc was overexpressed by 2- to 3-fold (Fig. 4E), showed augmented insulin secretion in their response to glucose (Fig. 4F) and increased insulin content at a steady state (Fig. 4G). While the expression levels of genes involved in glycolysis and ATP production were not changed, the mRNA levels of *Ins1* and *Ins2* were significantly up-regulated by the overexpression of NRDc in INS 832/13 cells (Fig. 4H). Notably, MafA expression was upregulated at the mRNA level (Fig. 4H) and the protein level in the nucleus (Fig. 4E). To ascertain whether NRDc regulates insulin expression through MafA, we performed gene knockdown of *Mafa* in NRDc-overexpressed INS 832/13 cells. *Mafa* knockdown did not affect the NRDc expression, whereas it canceled the augmentation of *Mafa* expression by NRDc overexpression (Fig. 5A). As a result, *Mafa* knockdown almost fully cancelled the NRDc-mediated increase of *Ins2* and partially cancelled the NRDc-mediated increase of *Ins1* gene expression (Fig. 5B). Thus, NRDc regulates insulin production, at least in part, by controlling MafA expression.

NRDc regulates the recruitment of Islet-1 to the MafA enhancer region

Previous reports showed that MafA expression is regulated by roughly 10 kilo-base pairs (bp) 5` of the transcription start site, which contain six highly conserved sequence domains, termed Regions 1–6 (33, 34). Among them, Region 3 (R3; -8118/-

7750 bp) has been reported to be essential for the expression of MafA in β-cells both *in vitro* and *in vivo* (33, 34). Several β-cell-enriched transcriptional factors, such as Pdx1, NeuroD1, NKx2.2, Islet-1, HNF1a, HNF1b, FoxA2 and NKx6.1, have their consensus binding motifs in R3 (35). Our chromatin immunoprecipitation (ChIP) assay using anti-mouse NRDc monoclonal antibody showed that NRDc is recruited to R3 of the MafA promoter in a mouse β-cell line, MIN6 cells (Fig. 6A). Furthermore, luciferase reporter assay showed that the gene knockdown of NRDc reduced the enhancer activity of R3 in MIN6 cells (Fig. 6B). As NRDc has no canonical DNA-binding motifs, we hypothesized that NRDc forms a complex with other transcription factors and exists on R3. To this end, we performed co-precipitation assays using cells overexpressing NRDc and Pdx1, NeuroD1, NKx2.2, Islet-1, HNF1a, HNF1b, FoxA2 or NKx6.1, and found that Islet-1 forms a complex with NRDc (Fig. 6C and data not shown).

As ChIP analysis indicated that both NRDc (Fig. 6A) and Islet-1 (Supplementary Fig. 5D) exist on R3 of the MafA promoter, we performed sequential ChIP-reChIP analysis to determine the *in vivo* colocalization of NRDc and Islet-1. As shown in Fig. 6D, ChIP-reChIP analysis with anti-NRDc and Islet-1 antibodies demonstrated that NRDc and Islet-1 are colocalized in R3 of the MafA promoter. To determine whether NRDc affects the recruitment of Islet-1 to R3, we performed ChIP analysis using MIN6 cells in which NRDc was knocked down (Fig. 6E, F). In consistent with results in *Nrd1*^{delβ} islets, gene knockdown of NRDc resulted in the decrease of MafA at the protein and mRNA levels (Fig. 6E, F). Intriguingly, gene knockdown of NRDc significantly reduced the recruitment of Islet-1, but not Pdx-1 and NeuroD1 to

R3 (Fig. 6G). Of note, gene knockdown of NRDc did not change the nuclear expression level of Islet-1 (Fig. 6E). Given the critical roles of Islet-1 in MafA regulation and β-cell function, our results suggest that NRDc regulates β-cell function, at least partially, through controlling the recruitment of Islet-1 to R3 of the MafA promoter.

Besides its transcriptional co-regulator function in the nucleus, NRDc enhances ectodomain shedding of membrane proteins (e.g. HB-EGF, TNF-α) through the activation of ADAMs (a disintegrin and metalloproteinase) (16-20). By immunoblotting and immunostaining in pancreatic β-cell lines (Fig. 4A, 4E, 6E and Supplementary Fig. 5A) and immunostaining in the islets of wild-type mice and human (Supplementary Fig. 5B, C), we demonstrate the intra- and extra-nuclear localization of NRDc in pancreatic β-cells. Broad spectrum ADAM and MMP inhibitor GM6001 blocks the activity of extracellular NRDc from enhancing ectodomain shedding (26). As shown in Supplementary Fig. 5E, GM6001 had no effect on the augmentation of *Mafa* expression by NRDc overexpression, suggesting that NRDc in the extracellular space has little, if any, effect on the transcription of MafA.

Acidic domain of NRDc is responsible for Islet-1 interaction and insulin production

One unique characteristic of NRDc among the M16 family of metalloendopeptidases is a highly acidic domain next to the catalytic domain (Fig. 7A), which is required for its binding to several proteins including HB-EGF, but dispensable for its metalloendopeptidase activity (36, 37). We transfected the mutant form of NRDc

lacking this acidic domain (dAcD) into *Nrd1*-/- MEF cells and tested whether the mutant interacts with Islet-1. Co-immunoprecipitation assays revealed that the acidic domain is responsible for the interaction between NRDc and Islet-1. On the other hand, the enzymatic activity of NRDc was dispensable for its binding to Islet-1 (Fig. 7A, B).

Islet-1 is a member of the LIM-homeodomain (LIM-HD) protein family, which is characterized by two tandemly arrayed LIM domains at the N terminus, a DNA-binding homeodomain and a LIM homeobox protein 3-binding domain (LBD) at the C terminus (Fig. 7C). To examine which domain of Islet-1 is required for the interaction with NRDc, we performed co-precipitation assays of NRDc and two deletion mutant forms of Islet-1 (Fig. 7C). The mutant Islet-1 lacking the N-terminal LIM domain (Islet-1^{delLIM}) showed markedly reduced co-precipitation with NRDc, while the mutant without the C-terminal LBD domain (Islet-1^{delC}) showed results similar to the wild type of Islet-1 (Fig. 7D). Collectively, these results indicated that the acidic domain of NRDc and the LIM domain of Islet-1 are responsible for their interaction.

To assess the functional significance of NRDc and Islet-1 interaction in pancreatic β-cells, we overexpressed the wild-type NRDc or the mutants of NRDc in INS 832/13 cells and examined NRDc-mediated augmentation of *Mafa* gene expression. Consistent with the results of co-precipitation assays, mRNA levels of *Mafa* were augmented by the wild type of NRDc, but not by NRDc lacking the highly acidic domain (Fig. 7E). Furthermore, induction of the *Ins1* mRNA level by NRDc expression was significantly reduced by the co-expression of dAcD mutant. On the other hand, islet1-induced upregulation of *Mafa* and *Ins1* mRNA levels was decreased by the

expression of Islet-1^{delLIM} (Fig. 7F). These results suggest that the interaction of NRDc and Islet-1 is required for the proper transcriptional regulation of *Mafa* and *Ins1*.

Although the enzymatically inactive E>A mutant bound to Islet-1 as the wild type of NRDc did (Fig. 7B), transcriptional induction of *Mafa* was not recapitulated by the E>A mutant (Fig. 7E). These results indicate that not only physical association between NRDc and Islet-1 but also enzymatic activity of NRDc appears to be involved in *Mafa, Ins1* and *Ins2* regulation.

DISCUSSION

In this report, we present the first *in vivo* evidence that NRDc is essential for proper β-cell function, especially for GSIS. *Nrd1*$^{-/-}$ mice develop glucose intolerance and severely impaired GSIS. Although the expression of NRDc is widespread in the whole body, the analysis of islets isolated from *Nrd1*$^{-/-}$ mice and β-cell-specific *Nrd1*-deficient mice clearly indicates that NRDc in β-cells is critical for insulin production and secretion. Accumulating evidence supports the notion that several β-cell-enriched transcription factors, such as Pdx-1, Nkx6.1 and MafA, play essential roles in the maintenance of β-cell function. Among them, MafA was solely downregulated in islets from *Nrd1*^{delβ} mice. Furthermore, *Mafa* mRNA level was increased by the overexpression of NRDc, while it was decreased by the gene knockdown of NRDc in β-cell lines, indicating that NRDc is a cell-autonomous regulator of MafA transcription. Importantly, NRDc overexpression in INS 832/13 cells was accompanied by increased mRNA levels and the secretion of insulin, which was partially inhibited by the simultaneous gene knockdown of *Mafa*. These results demonstrated that NRDc regulates insulin production and GSIS through the control of MafA expression.

MafA is first produced at E13.5 exclusively in insulin-positive cells, which is unusually late compared with other islet-enriched transcription factors (38). Moreover, *Mafa* mRNA levels show an age-dependent increase from neonates to adults, which is similar to the expression pattern of insulin and other putative target genes of MafA (39). This unique spatial and temporal expression pattern of MafA is regulated by its well-

established 5' flanking enhancer region, called Region 3 (R3; -8118/-7750 bp) (34, 40). We show here that NRDc binds to the MafA enhancer R3. We also demonstrated that the enhancer activity of MafA R3 is reduced by the gene knockdown of NRDc. In addition, we performed unbiased screening of β-cell-enriched transcriptional factors for binding to NRDc, and found that Islet-1 associates with NRDc. Notably, ChIP-reChIP assay clearly demonstrated the association of NRDc and Islet-1 in the MafA enhancer R3. Furthermore, gene knockdown of NRDc was accompanied by the decrease of Islet-1 recruitment to R3. Given that MafA is a direct target of Islet-1, MafA regulation by NRDc is, at least partially, attributed to the NRDc-mediated Islet-1 recruitment to the MafA enhancer.

We show that the acidic domain of NRDc and the LIM domain of Islet-1 are required not only for complex formation but also for the full enhancement of *Mafa* and *Ins1* mRNA. Islet-1 is a member of the LIM-homeodomain protein family, characterized by two tandemly repeated LIM domains fused to a conserved homeodomain. The LIM domain consists of two tandemly repeated zinc fingers, structurally similar to GATA-type zinc fingers (41). However, unlike GATA-type zinc fingers, the LIM domain in mammalian LIM proteins does not seem to bind to DNA. Instead, the domain appears to be important for the diverse protein-protein interactions (42). Two transcription factors, LIM-domain-binding protein 1 (43) and NeuroD (44), were previously reported to bind islet-1 via the LIM domain and activate the transcriptional activity of Islet-1. Meanwhile, the deletion of the LIM domains from Islet-1 was reported to enhance the insulin-promoter-driven luciferase activity in HEK-

293 cells (44). As opposed to that result, the LIM domain-deleted mutant of Islet-1, overexpressed in INS832/13 cells, failed to elevate the mRNA levels of *Mafa* and *Ins1*. Although these findings are inconsistent, our results in β-cells are more likely to recapitulate the physiological regulation of insulin promoter activity. Some factors in β-cells, such as NeuroD and NRDc, may activate the transcription of insulin through interacting with the LIM domains.

Although both *Nrd1*$^{-/-}$ and *Nrd1*^{delβ} mice show glucose intolerance and severely impaired GSIS, there are some differences between these two mouse lines. First, fasting blood glucose was normal in *Nrd1*$^{-/-}$ mice, while it was elevated in *Nrd1*^{delβ} mice. Second, β-cell mass was unaltered in *Nrd1*$^{-/-}$ mice, but reduced in *Nrd1*^{delβ} mice. Third, the α-cell/β-cell ratio was unchanged in *Nrd1*$^{-/-}$ mice, but significantly increased in *Nrd1*^{delβ} mice. *Nrd1*^{delβ} mice also showed the dysregulated distribution patterning of glucagon-positive α-cells, a phenotype that is similar to that of *Mafa*-deficient mice (9). Consistently, *Nrd1*^{delβ} mice showed hyperglucagonemia. Considering that insulin sensitivity was enhanced in *Nrd1*$^{-/-}$ mice, hyperglucagonemia and unaltered insulin sensitivity in *Nrd1*^{delβ} mice may account for their severe glucose intolerance. Insulin hypersensitivity in *Nrd1*$^{-/-}$ mice may arise from an increase in energy expenditure due to enhanced thermogenesis in brown adipose tissue and elevated physical activity (21). Our ongoing studies using organ-specific (e.g. liver, adipose tissue and skeletal muscle) NRDc-deficient mice will further clarify the role of NRDc in the regulation of insulin sensitivity.

Recent reports have indicated that several transcription factors, such as Pdx1 (6), Nkx6.1 (7) and FoxO1 (45), are critical for β-cells to maintain their differentiated states. Loss of FoxO1 in mature β-cells leads to the dedifferentiation of β-cells, characterized by upregulation of *Ngn3,* the endocrine progenitor cell marker. A subset of dedifferentiated cells was shown to adopt an α-cell fate (45). Importantly, possible dedifferentiation and the conversion of β-cells to α-cells have also been reported in *Mafa*-deficient mice (46). Our results of lineage tracing experiments demonstrated that a small portion of glucagon-positive cells in *Nrd1*$^{del\beta}$ islets originated from β-cells. Moreover, endocrine progenitor cell marker, such as *Sox9*, *Ngn3, Mafb* and *Aldh1a3* (47), were upregulated in *Nrd1*$^{del\beta}$ islets. Together, these results suggest that the dedifferentiation of β-cells and redifferentiation to the glucagon-expressing α-like cells might occur in a subset of β-cells in an islet environment where NRDc-positive α-cells and NRDc-negative β-cells are intermingled. As the β-to-α conversion in *Nrd1*$^{del\beta}$ islets was observed in only a limited number of cells (3.28% of the total glucagon-positive cells), reduced β-cell proliferation, a phenotype observed in MafA-depleted β-cells (48, 49), may account for the increased α-cell/β-cell ratio in *Nrd1*$^{del\beta}$ islets. Meanwhile, *Glut2*–deficient mice also display the increased α-cell/β-cell ratio, although the mechanism is elusive (50). As mRNA and protein expressions of GLUT2 were clearly reduced in *Nrd1*$^{del\beta}$ islets, NRDc might modulate α-cell/β-cell ratio via the regulation of *Glut2* in *Nrd1*$^{del\beta}$ islets. Interestingly, *Glut2*–deficient mice (50, 51) and/or transgenic mice expressing the glucose-sensor-dead mutant of GLUT2 (52) share several phenotypes with *Nrd1*$^{del\beta}$ mice; a reduction in pancreatic insulin content, basal and

glucose-stimulated insulin secretion, an increased α-cell/β-cell ratio, and increased ratio of small islets. Future studies using *Glut2*-rescued *Nrd1*^{delβ} mice might clarify the precise role of *Glut2* in the regulation of β-cell function and proliferation by NRDc.

NRDc in the nucleus has been identified as a histone-binding protein, specifically recognizing dimethyl-H3K4 (22). The roles of NRDc in transcriptional regulation have been illustrated by the interaction of NRDc with various nuclear proteins such as HDAC3 in the NCoR/SMRT complex and PGC-1α (21, 22). We demonstrate here that Islet-1 is a novel binding partner of NRDc in β-cells. Considering the context-dependent multiple binding partners and wide range of phenotypes of *Nrd1*$^{-/-}$ mice (19, 21, 53), NRDc may function as a transcriptional coregulator in general. Since NRDc has its own peptidase activity, which seems to be involved in MafA regulation, further study using peptidase-dead mutant knockin mice will be required to clarify the link between the biological role and the protein function of NRDc.

Acknowledgments

We are grateful to H. Iwai, K. Shimada, and N. Nishimoto (Kyoto University) for technical assistance, C.B. Newgard (Duke University), J. Miyazaki (Osaka University), T. Masui and, A. Sato (Kyoto University) for materials.

Funding

This study was supported by research grants (26293068, 26670139, 26116715, 15K19376, 15K19513 and 16K15216) and a research program of the Project for Development of Innovative Research on Cancer Therapeutics (P-Direct) from the Ministry of Education, Culture, Sports, Science and Technology of Japan. It was also supported by a Health Labour Sciences Research Grant from the Ministry of Health, Labour and Welfare (Comprehensive Research on Lifestyle-Related Diseases including Cardiovascular Diseases and Diabetes Mellitus), the Takeda Science Foundation, the Mitsui Sumitomo Insurance Welfare Foundation, Kao Research Council for the Study of Healthcare Science, The Uehara Memorial Foundation and the Otsuka Pharmaceutical Co., Ltd. Sponsored Research Program.

Duality of Interest

No potential conflicts of interest relevant to this article were reported

AUTHOR CONTRIBUTIONS

K.N. and E.N. designed experiments and wrote the manuscript. K.N., M.O., Y.H., S.S.,

J.S., PM.C., Y.M. and S.M. performed experiments and analyzed data. Y.S., K.I., K.S., N.H. and N.I. performed islet isolation and insulin secretion assay. Y.M. and H.K. generated *Nrd1*$^{flox/flox}$ mice. K.F., Y.K. and S.U. carried out the histological procedures and provided human samples. Y.K, N.I., T.Kita and T.Kimura supervised the work. E.N. is the guarantor of this work and, as such, had full access to all the data in the study and takes responsibility for the integrity of the data and the accuracy of the data analysis.

REFERENCES

1. Ashcroft FM, Rorsman P: Diabetes mellitus and the beta cell: the last ten years. Cell 2012;148:1160-1171

2. Muoio DM, Newgard CB: Mechanisms of disease:Molecular and metabolic mechanisms of insulin resistance and beta-cell failure in type 2 diabetes. Nat Rev Mol Cell Biol 2008;9:193-205

3. Hasnain SZ, Prins JB, McGuckin MA: Oxidative and endoplasmic reticulum stress in beta-cell dysfunction in diabetes. J Mol Endocrinol 2016;56:R33-54

4. Guo S, Dai C, Guo M, Taylor B, Harmon JS, Sander M, Robertson RP, Powers AC, Stein R: Inactivation of specific beta cell transcription factors in type 2 diabetes. J Clin Invest 2013;123:3305-3316

5. Ahlgren U, Jonsson J, Jonsson L, Simu K, Edlund H: beta-cell-specific inactivation of the mouse Ipf1/Pdx1 gene results in loss of the beta-cell phenotype and maturity onset diabetes. Genes Dev 1998;12:1763-1768

6. Gao T, McKenna B, Li C, Reichert M, Nguyen J, Singh T, Yang C, Pannikar A, Doliba N, Zhang T, Stoffers DA, Edlund H, Matschinsky F, Stein R, Stanger BZ: Pdx1 Maintains beta Cell Identity and Function by Repressing an alpha Cell Program. Cell Metab 2014;19:259-271

7. Taylor BL, Liu FF, Sander M: Nkx6.1 is essential for maintaining the functional state of pancreatic beta cells. Cell Rep 2013;4:1262-1275

8. Kataoka K, Han SI, Shioda S, Hirai M, Nishizawa M, Handa H: MafA is a glucose-regulated and pancreatic beta-cell-specific transcriptional activator for the insulin gene. J Biol Chem 2002;277:49903-49910

9. Zhang C, Moriguchi T, Kajihara M, Esaki R, Harada A, Shimohata H, Oishi H,

Hamada M, Morito N, Hasegawa K, Kudo T, Engel JD, Yamamoto M, Takahashi S: MafA is a key regulator of glucose-stimulated insulin secretion. Mol Cell Biol 2005;25:4969-4976

10. Gu C, Stein GH, Pan N, Goebbels S, Hornberg H, Nave KA, Herrera P, White P, Kaestner KH, Sussel L, Lee JE: Pancreatic beta cells require NeuroD to achieve and maintain functional maturity. Cell Metab 2010;11:298-310

11. Ediger BN, Du A, Liu J, Hunter CS, Walp ER, Schug J, Kaestner KH, Stein R, Stoffers DA, May CL: Islet-1 Is essential for pancreatic beta-cell function. Diabetes 2014;63:4206-4217

12. Du A, Hunter CS, Murray J, Noble D, Cai CL, Evans SM, Stein R, May CL: Islet-1 is required for the maturation, proliferation, and survival of the endocrine pancreas. Diabetes 2009;58:2059-2069

13. Chesneau V, Pierotti AR, Barre N, Creminon C, Tougard C, Cohen P: Isolation and characterization of a dibasic selective metalloendopeptidase from rat testes that cleaves at the amino terminus of arginine residues. J Biol Chem 1994;269:2056-2061

14. Pierotti AR, Prat A, Chesneau V, Gaudoux F, Leseney AM, Foulon T, Cohen P: N-arginine dibasic convertase, a metalloendopeptidase as a prototype of a class of processing enzymes. Proc Natl Acad Sci U S A 1994;91:6078-6082

15. Nishi E, Prat A, Hospital V, Elenius K, Klagsbrun M: N-arginine dibasic convertase is a specific receptor for heparin-binding EGF-like growth factor that mediates cell migration. EMBO J 2001;20:3342-3350

16. Hiraoka Y, Ohno M, Yoshida K, Okawa K, Tomimoto H, Kita T, Nishi E: Enhancement of alpha-secretase cleavage of amyloid precursor protein by a metalloendopeptidase nardilysin. J Neurochem 2007;102:1595-1605

17. Hiraoka Y, Yoshida K, Ohno M, Matsuoka T, Kita T, Nishi E: Ectodomain shedding of TNF-alpha is enhanced by nardilysin via activation of ADAM proteases. Biochem Biophys Res Commun 2008;370:154-158

18. Nishi E, Hiraoka Y, Yoshida K, Okawa K, Kita T: Nardilysin enhances ectodomain shedding of heparin-binding epidermal growth factor-like growth factor through activation of tumor necrosis factor-alpha-converting enzyme. J Biol Chem 2006;281:31164-31172

19. Ohno M, Hiraoka Y, Matsuoka T, Tomimoto H, Takao K, Miyakawa T, Oshima N, Kiyonari H, Kimura T, Kita T, Nishi E: Nardilysin regulates axonal maturation and myelination in the central and peripheral nervous system. Nat Neurosci 2009;12:1506-1513

20. Ohno M, Hiraoka Y, Lichtenthaler SF, Nishi K, Saijo S, Matsuoka T, Tomimoto H, Araki W, Takahashi R, Kita T, Kimura T, Nishi E: Nardilysin prevents amyloid plaque formation by enhancing alpha-secretase activity in an Alzheimer's disease mouse model. Neurobiol Aging 2014;35:213-222

21. Hiraoka Y, Matsuoka T, Ohno M, Nakamura K, Saijo S, Matsumura S, Nishi K, Sakamoto J, Chen PM, Inoue K, Fushiki T, Kita T, Kimura T, Nishi E: Critical roles of nardilysin in the maintenance of body temperature homoeostasis. Nat Commun 2014;5:3224

22. Li J, Chu M, Wang S, Chan D, Qi S, Wu M, Zhou Z, Li J, Nishi E, Qin J, Wong J: Identification and characterization of nardilysin as a novel dimethyl H3K4-binding protein involved in transcriptional regulation. J Biol Chem 2012;287:10089-10098

23. Yagi T, Tokunaga T, Furuta Y, Nada S, Yoshida M, Tsukada T, Saga Y, Takeda N, Ikawa Y, Aizawa S: A novel ES cell line, TT2, with high germline-differentiating potency. Anal Biochem 1993;214:70-76

24. Postic C, Shiota M, Niswender KD, Jetton TL, Chen Y, Moates JM, Shelton KD, Lindner J, Cherrington AD, Magnuson MA: Dual roles for glucokinase in glucose homeostasis as determined by liver and pancreatic beta cell-specific gene knock-outs using Cre recombinase. J Biol Chem 1999;274:305-315

25. Hohmeier HE, Mulder H, Chen G, Henkel-Rieger R, Prentki M, Newgard CB: Isolation of INS-1-derived cell lines with robust ATP-sensitive K+ channel-dependent and -independent glucose-stimulated insulin secretion. Diabetes 2000;49:424-430

26. Moss ML, Rasmussen FH: Fluorescent substrates for the proteinases ADAM17, ADAM10, ADAM8, and ADAM12 useful for high-throughput inhibitor screening. Anal Biochem 2007;366:144-148

27. Yoshihara E, Fujimoto S, Inagaki N, Okawa K, Masaki S, Yodoi J, Masutani H: Disruption of TBP-2 ameliorates insulin sensitivity and secretion without affecting obesity. Nat Commun 2010;1:127

28. Sato Y, Fujimoto S, Mukai E, Sato H, Tahara Y, Ogura K, Yamano G, Ogura M, Nagashima K, Inagaki N: Palmitate induces reactive oxygen species production and beta-cell dysfunction by activating nicotinamide adenine dinucleotide phosphate oxidase through Src signaling. J Diabetes Investig 2014;5:19-26

29. Miyazaki J, Araki K, Yamato E, Ikegami H, Asano T, Shibasaki Y, Oka Y, Yamamura K: Establishment of a pancreatic beta cell line that retains glucose-inducible insulin secretion: special reference to expression of glucose transporter isoforms. Endocrinology 1990;127:126-132

30. Lee JY, Ristow M, Lin X, White MF, Magnuson MA, Hennighausen L: RIP-Cre revisited, evidence for impairments of pancreatic beta-cell function. J Biol Chem 2006;281:2649-2653

31. Srinivas S, Watanabe T, Lin CS, William CM, Tanabe Y, Jessell TM, Costantini F:

Cre reporter strains produced by targeted insertion of EYFP and ECFP into the ROSA26 locus. BMC Dev Biol 2001;1:4

32. Hoang Do O, Thorn P: Insulin secretion from beta cells within intact islets: location matters. Clin Exp Pharmacol Physiol 2015;42:406-414

33. Raum JC, Gerrish K, Artner I, Henderson E, Guo M, Sussel L, Schisler JC, Newgard CB, Stein R: FoxA2, Nkx2.2, and PDX-1 regulate islet beta-cell-specific mafA expression through conserved sequences located between base pairs -8118 and -7750 upstream from the transcription start site. Mol Cell Biol 2006;26:5735-5743

34. Raum JC, Hunter CS, Artner I, Henderson E, Guo M, Elghazi L, Sosa-Pineda B, Ogihara T, Mirmira RG, Sussel L, Stein R: Islet beta-cell-specific MafA transcription requires the 5'-flanking conserved region 3 control domain. Mol Cell Biol 2010;30:4234-4244

35. Hunter CS, Stein R: Characterization of an apparently novel beta-cell line-enriched 80-88 kDa transcriptional activator of the MafA and Pdx1 genes. J Biol Chem 2013;288:3795-3803

36. Hospital V, Nishi E, Klagsbrun M, Cohen P, Seidah NG, Prat A: The metalloendopeptidase nardilysin (NRDc) is potently inhibited by heparin-binding epidermal growth factor-like growth factor (HB-EGF). Biochem J 2002;367:229-238

37. Nishi E: Chapter 319 - Nardilysin. In Handbook of Proteolytic Enzymes Salvesen NDR, Ed., Academic Press, 2013, p. 1421-1426

38. Matsuoka TA, Artner I, Henderson E, Means A, Sander M, Stein R: The MafA transcription factor appears to be responsible for tissue-specific expression of insulin. Proc Natl Acad Sci U S A 2004;101:2930-2933

39. Aguayo-Mazzucato C, Koh A, El Khattabi I, Li WC, Toschi E, Jermendy A, Juhl K, Mao K, Weir GC, Sharma A, Bonner-Weir S: Mafa expression enhances glucose-responsive insulin secretion in neonatal rat beta cells. Diabetologia 2011;54:583-593

40. Hang Y, Stein R: MafA and MafB activity in pancreatic beta cells. Trends Endocrinol Metab 2011;22:364-373

41. Perez-Alvarado GC, Miles C, Michelsen JW, Louis HA, Winge DR, Beckerle MC, Summers MF: Structure of the carboxy-terminal LIM domain from the cysteine rich protein CRP. Nat Struct Biol 1994;1:388-398

42. Bach I: The LIM domain: regulation by association. Mech Dev 2000;91:5-17

43. Jurata LW, Gill GN: Functional analysis of the nuclear LIM domain interactor NLI. Mol Cell Biol 1997;17:5688-5698

44. Zhang H, Wang WP, Guo T, Yang JC, Chen P, Ma KT, Guan YF, Zhou CY: The LIM-homeodomain protein ISL1 activates insulin gene promoter directly through synergy with BETA2. J Mol Biol 2009;392:566-577

45. Talchai C, Xuan S, Lin HV, Sussel L, Accili D: Pancreatic beta cell dedifferentiation as a mechanism of diabetic beta cell failure. Cell 2012;150:1223-1234

46. Nishimura W, Takahashi S, Yasuda K: MafA is critical for maintenance of the mature beta cell phenotype in mice. Diabetologia 2015;58:566-574

47. Cinti F, Bouchi R, Kim-Muller JY, Ohmura Y, Rodrigo Sandoval P, Masini M, Marselli L, Suleiman M, Ratner LE, Marchetti P, Accili D: Evidence of β-cell Dedifferentiation in Human Type 2 Diabetes. The Journal of Clinical Endocrinology & Metabolism 2015:jc.2015-2860

48. Hang Y, Yamamoto T, Benninger RK, Brissova M, Guo M, Bush W, Piston DW,

Powers AC, Magnuson M, Thurmond DC, Stein R: The MafA transcription factor becomes essential to islet beta-cells soon after birth. Diabetes 2014;63:1994-2005

49. Eto K, Nishimura W, Oishi H, Udagawa H, Kawaguchi M, Hiramoto M, Fujiwara T, Takahashi S, Yasuda K: MafA is required for postnatal proliferation of pancreatic beta-cells. PLoS One 2014;9:e104184

50. Guillam MT, Dupraz P, Thorens B: Glucose uptake, utilization, and signaling in GLUT2-null islets. Diabetes 2000;49:1485-1491

51. Guillam MT, Hummler E, Schaerer E, Yeh JI, Birnbaum MJ, Beermann F, Schmidt A, Deriaz N, Thorens B: Early diabetes and abnormal postnatal pancreatic islet development in mice lacking Glut-2. Nat Genet 1997;17:327-330

52. Stolarczyk E, Le Gall M, Even P, Houllier A, Serradas P, Brot-Laroche E, Leturque A: Loss of sugar detection by GLUT2 affects glucose homeostasis in mice. PLoS One 2007;2:e1288

53. Ishizu-Higashi S, Seno H, Nishi E, Matsumoto Y, Ikuta K, Tsuda M, Kimura Y, Takada Y, Kimura Y, Nakanishi Y, Kanda K, Komekado H, Chiba T: Deletion of nardilysin prevents the development of steatohepatitis and liver fibrotic changes. PLoS One 2014;9:e98017

Figure Legends

Figure 1. *Nrd1*$^{-/-}$ mice and islets exhibit impaired glucose-stimulated insulin secretion (GSIS).

(A, B) Glucose tolerance test (i.p. injection of 2 mg/kg glucose) reveals mild glucose intolerance (A) and impaired insulin secretion (B) in 3-month-old *Nrd1*$^{-/-}$ mice (n=7-10 per genotype).

(C) Insulin tolerance test (i.p. injection of 1 U/kg insulin) reveals increased insulin sensitivity in 3-month-old *Nrd1*$^{-/-}$ mice (n=4 per genotype).

(D) Pancreata from 3-month-old *Nrd1*$^{+/+}$ and *Nrd1*$^{-/-}$ mice were stained with anti-insulin (red) and anti-glucagon (green) antibodies.

(E) β-cell (insulin-positive cell) mass/body weight is not changed in *Nrd1*$^{-/-}$ mice (n=4 per genotype).

(F) Proportion of α-cell (glucagon-positive cell) areas among α- and β-cell (insulin-positive cell) areas is not changed in *Nrd1*$^{-/-}$ mice (n=4 per genotype).

(G) Static incubation of islets from 3- to 4-month-old *Nrd1*$^{+/+}$ and *Nrd1*$^{-/-}$ mice with 2.8 mM glucose, 25 mM glucose, and 30mM KCl. Secreted insulin was normalized to total insulin in the islets (n=20 per group).

(H) Insulin contents normalized to protein concentration in isolated islets are reduced in *Nrd1*$^{-/-}$ mice (n=20 per genotype).

(I) Proinsulin/insulin ratio is not changed in *Nrd1*$^{-/-}$ mice (n=5-8 per genotype).

* $p<0.05$, ** $p<0.01$, NS: not significant.

Figure 2. β-cell-specific NRDc-deficient (*Nrd1*^{delβ}) mice show diabetic phenotype with markedly reduced GSIS.

(A) Fasting hyperglycemia in 6-month-old *Nrd1*^{delβ} mice (n=9-14 per genotype).

(B, C) Glucose tolerance test (i.p. injection of 2 mg/kg glucose) reveals glucose intolerance (B) and impaired insulin secretion (C) in 6-month-old *Nrd1*^{delβ} mice (n=4-8 per genotype). * $p<0.05$ for *Nrd1*^{delβ} vs. Rip-cre, # $p<0.05$ for *Nrd1*^{delβ} vs. Floxed, ## $p<0.01$ for *Nrd1*^{delβ} vs. Floxed, † $p<0.05$ for Rip-cre vs. Floxed.

(D) Pancreata from 6-month-old *Nrd1*^{delβ} and control mice were stained with anti-insulin (red) and anti-glucagon (green) antibodies.

(E) Proportion of glucagon-positive areas among glucagon- and insulin-positive areas is increased in *Nrd1*^{delβ} mice (n=4 per genotype).

(F) Fasting hyperglucagonemia in 6-month-old *Nrd1*^{delβ} mice (n=5-6 per genotype).

(G) Relative mRNA levels of *glucagon* in isolated islets from 6-month-old Nrd1^{delβ} and control mice, as measured by qRT-PCR (n=4-5 per genotype).

(H) Quantification of β-cell (insulin-positive cell) mass in 6-month-old *Nrd1*^{delβ} and control mice (n=4 per genotype).

(I) Distribution of islet size in 6-month-old *Nrd1*^{delβ} and control mice (n=4 per genotype).

* $p<0.05$, ** $p<0.01$, *** $p<0.001$, unless otherwise noted.

Figure 3. Islets from *Nrd1*^{delβ} mice exhibit reduced GSIS with decreased MafA expression.

(A) Static incubation of islets from 6- to 8-month-old *Nrd1*^{delβ} and control mice with 2.8 mM and 25 mM glucose. Secreted insulin was normalized to total insulin in the islets (n=10 per group).

(B) Insulin contents normalized to protein concentration in isolated islets are reduced in *Nrd1*^{delβ} mice (n=10 per group).

(C, D) Relative mRNA levels of genes involved in insulin secretion (C) and transcriptional factors (D) in islets isolated from 6-month-old *Nrd1*^{delβ} and RIP-cre mice, as measured by qRT-PCR (n=4-5 per genotype).

(E) Pancreata from 6-month-old *Nrd1*^{delβ} and control mice were stained with anti-GLUT2 (red) and anti-insulin (green) antibodies.

(F) Pancreata from 6-month-old *Nrd1*^{delβ} and control mice were stained with anti-MafA (red) and anti-insulin (green) antibodies.

* $p<0.05$, ** $p<0.01$, *** $p<0.001$.

Figure 4. NRDc cell-autonomously regulates insulin secretion and MafA expression.

(A) Western blot analysis of cytosolic and nuclear fractions of INS 832/13 cells infected with miRs targeted to *Nrd1* or a control miR.

(B) Static incubation of INS 832/13 cells described in (A) with 2.8 mM and 15 mM glucose. Secreted insulin was normalized to protein concentration (n=9 per group).

(C) Insulin contents normalized to protein concentration in INS 832/13 cells described in (A) (n=4 per group).

(D) Relative mRNA levels of genes in INS 832/13 cells described in (A), as measured by qRT-PCR (n=4 per group).

(E) Western blot analysis of cytosolic and nuclear fractions of control or NRDc-overexpressing INS 832/13 cells using the indicated antibodies.

(F) Static incubation of control or NRDc-overexpressing INS 832/13 cells with 2.8 mM and 15 mM glucose. Secreted insulin was normalized to protein concentration (n=9 per group).

(G) Insulin contents normalized to protein concentration in control or NRDc-overexpressing INS 832/13 cells (n=6 per group).

(H) Relative mRNA levels of genes in control or NRDc-overexpressing INS 832/13 cells, as measured by qRT-PCR (n=5 per group).

* $p<0.05$, ** $p<0.01$, NS: not significant.

Figure 5. NRDc regulates insulin production through MafA.

(A) Relative mRNA levels of *Nrd1* and *Mafa* in control or NRDc-overexpressing INS 832/13 cells, in which *Mafa* is knocked down by microRNA (miR) targeted to *Mafa* (or a control miR). n=4 per group.

(B) Relative mRNA levels of *Ins1* and *Ins2* in INS 832/13 cells described in (A). Gene knockdown of *Mafa* reduces NRDc-mediated augmentation of *Ins1* gene expression in INS 832/13 cells. Relative ratios of *Ins1* and *Ins2* mRNA level in NRDc-overexpressing

cells to that in control cells are shown in the right panel (n=4 per group).

* $p<0.05$, ** $p<0.01$, NS: not significant.

Figure 6. NRDc regulates the recruitment of Islet-1 to the enhancer region of MafA.

(A) ChIP with anti-NRDc antibody followed by qRT-PCR demonstrates that NRDc binds to the enhancer region of MafA in MIN6 cells. Results were normalized with input DNA (n = 6). MafA R3: -8118 to -7750 relative to the transcriptional start site (TSS) of *Mafa*; Non-conserved: -1678 to -1560 relative to the TSS of *Mafa.*

(B) Luciferase activity was quantified in MIN6 cells 48 hours after the transfection of PGV-P2 with the insertion of MafA R3. The luciferase activity was normalized by the activity of PGV-P2 without MafA R3. (n=4).

(C) NRDc forms a complex with Islet-1. NRDc was co-transfected with FLAG-tagged Pdx1 (P), NeuroD1 (N), Islet-1 (I) or a control vector (-) into $NRDc^{-/-}$ MEFs. Arrows indicate non-specific bands.

(D) ChIP/re-ChIP analysis of MIN6 cells with anti-NRDc and Islet-1 antibodies followed by qRT-PCR targeting MafA R3 (n = 4).

(E) Western blot analysis of cytosolic and nuclear fractions of MIN6 cells infected with miRs targeted to *Nrd1* or a control miR.

(F) Relative mRNA levels of genes in MIN6 cells described in (D), as measured by qRT-PCR (n = 5).

(G) ChIP with antibodies to PDX-1, NeuroD and Islet-1 followed by qRT-PCR demonstrates that *Nrd1* knockdown in MIN6 cells decreases Islet-1 recruitment to MafA R3. The results were normalized to input DNA, and are shown as the ratio to that in the control miR-treated cells (IP: αPDX-1, αNeuroD or αIslet1) (n = 6).

* $p<0.05$, *** $p<0.001$.

Figure 7. Acidic domain of NRDc is responsible for its association with Islet-1 and insulin production.

(A) Schematics of the mutants of NRDc. E>A: the enzymatically inactive mutant. dAcD: the mutant lacking the highly acidic domain. AcD: Acidic domain, M16: Peptidase M16 domain.

(B) The highly acidic domain of NRDc is required for complex formation between NRDc and Islet-1. Wild-type NRDc or indicated mutants described in (A) were co-transfected with Islet-1 into $NRDc^{-/-}$ MEFs. Arrows indicate non-specific bands.

(C) Schematics of Islet-1 and deletion mutants. LIM1 and LIM2: first and second LIM domains, HD: homeo domain, LBD: Lhx3/4 binding domain.

(D) The LIM domain of Islet-1 is required for the complex formation between NRDc and Islet-1. FLAG-tagged wild-type Islet-1 or deletion mutants described in (C) were co-transfected with NRDc into $NRDc^{-/-}$ MEFs.

(E) Relative mRNA levels of *Nrd1*, *Mafa Ins1* and *Ins2* in INS 832/13 cells infected with wild-type or mutated NRDc (n=8 per group). Expression levels of the mock infected cells are normalized to 1.

(F) Relative mRNA levels of *Nrd1*, *Mafa Ins1* and *Ins2* in INS 832/13 cells infected with wild-type or mutated Islet-1 (n=5 per group). Expression levels of the mock infected cells are normalized to 1.

* $p<0.05$, ** $p<0.01$, *** $p<0.001$.

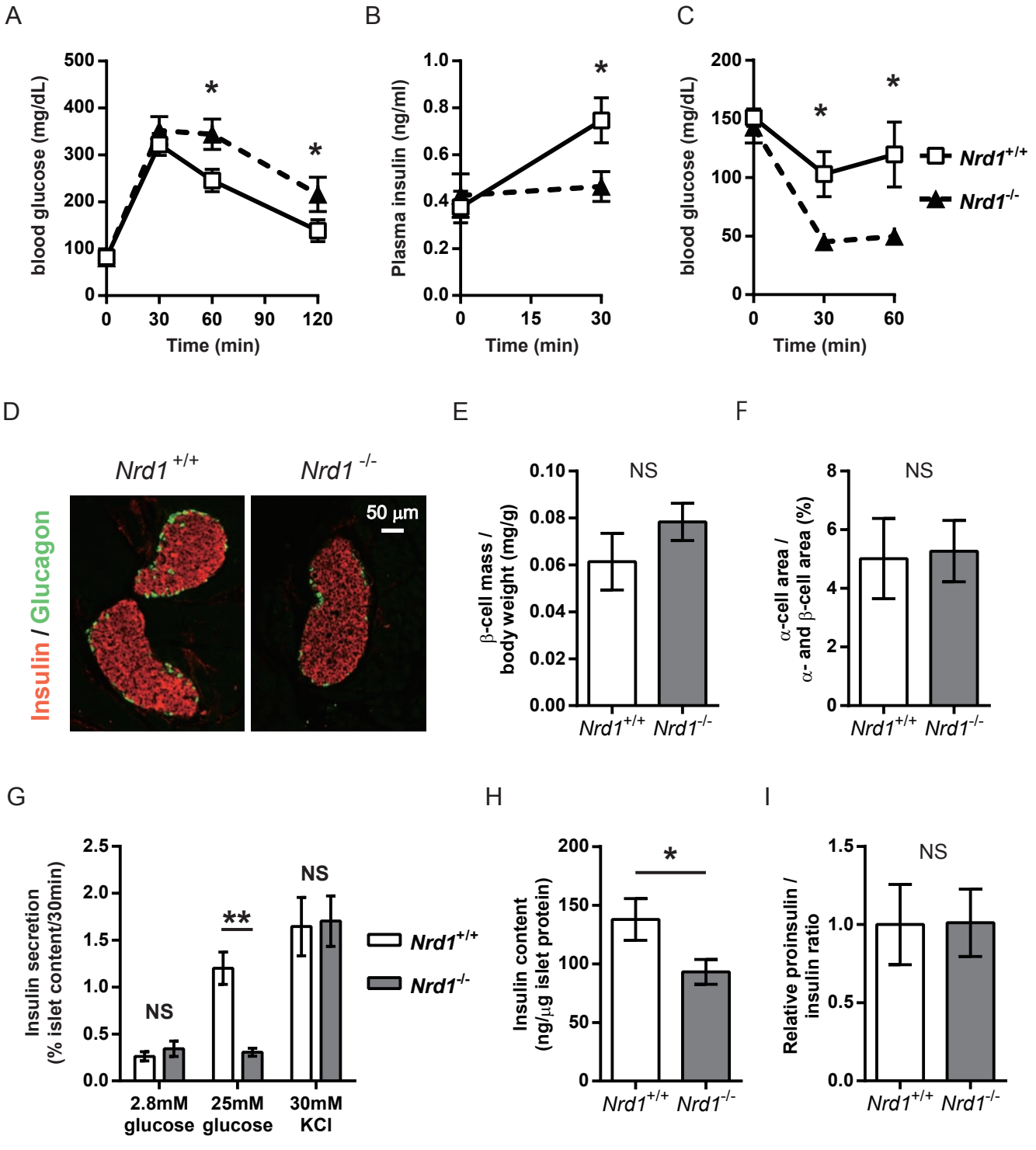
A
blood glucose (mg/dL)
Time (min)
B
Plasma insulin (ng/ml)
Time (min)
C
blood glucose (mg/dL)
Time (min)
Nrd1+/+
Nrd1-/-
D
Nrd1 +/+
Nrd1 -/-
Insulin / Glucagon
50 µm
E
β-cell mass / body weight (mg/g)
NS
F
α-cell area / α- and β-cell area (%)
NS
G
Insulin secretion (% islet content/30min)
NS
**
NS
2.8mM glucose
25mM glucose
30mM KCl
H
Insulin content (ng/µg islet protein)
*
I
Relative proinsulin / insulin ratio
NS

Figure 1

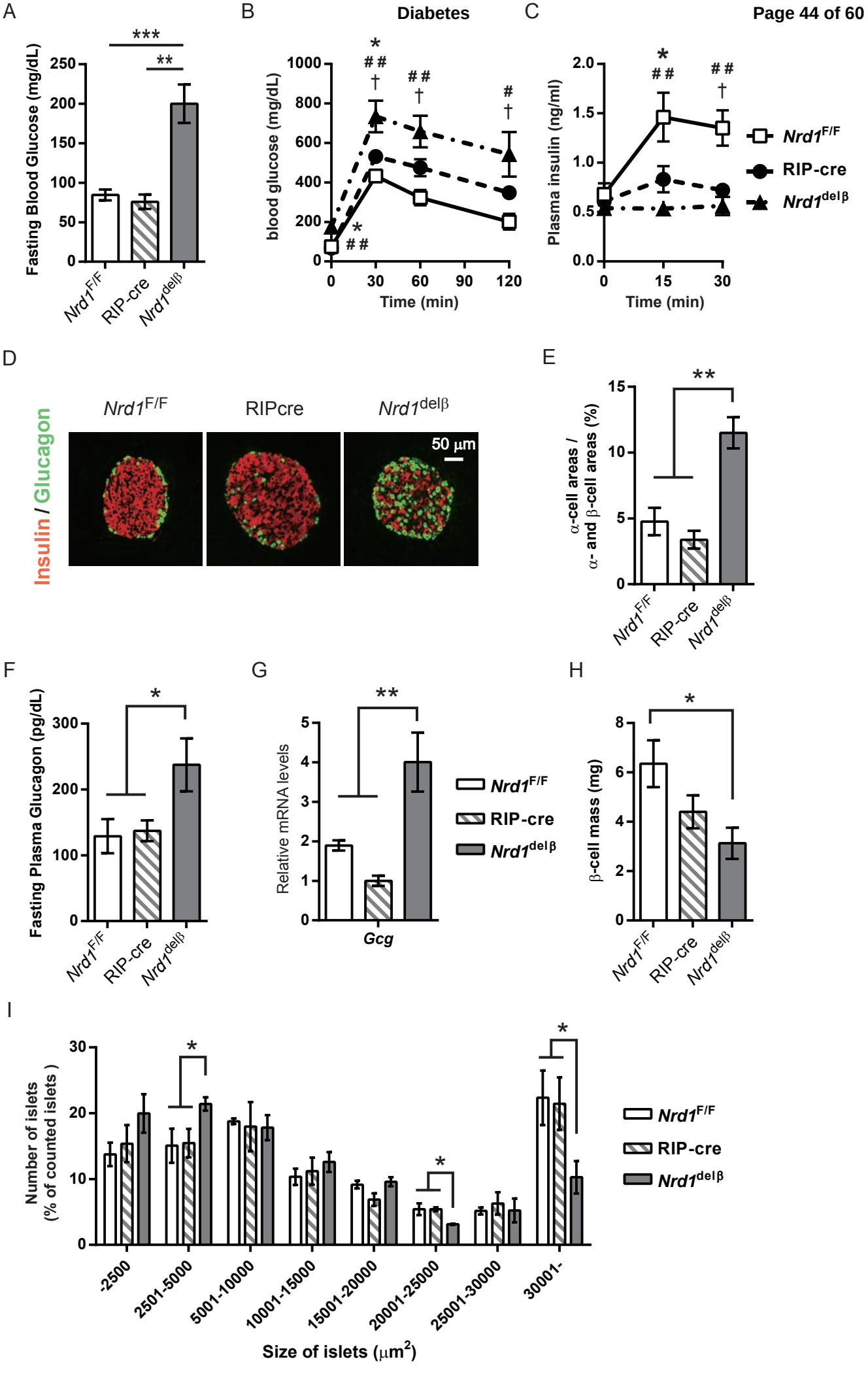
A
Fasting Blood Glucose (mg/dL)
250
200
150
100
50
0
***
**
Nrd1F/F
RIP-cre
Nrd1delβ
B
blood glucose (mg/dL)
1000
800
600
400
200
0
0
30
60
90
120
Time (min)
C
Plasma insulin (ng/ml)
2.0
1.5
1.0
0.5
0.0
0
15
30
Time (min)
Nrd1F/F
RIP-cre
Nrd1delβ
D
Nrd1F/F
RIPcre
Nrd1delβ
Insulin / Glucagon
50 µm
E
α-cell areas / α- and β-cell areas (%)
15
10
5
0
**
F
Fasting Plasma Glucagon (pg/dL)
300
200
100
0
*
G
Relative mRNA levels
5
4
3
2
1
0
**
Gcg
H
β-cell mass (mg)
8
6
4
2
0
*
I
Number of islets (% of counted islets)
30
20
10
0
*
*
*
-2500
2501-5000
5001-10000
10001-15000
15001-20000
20001-25000
25001-30000
30001-
Size of islets (µm2)

Figure 2

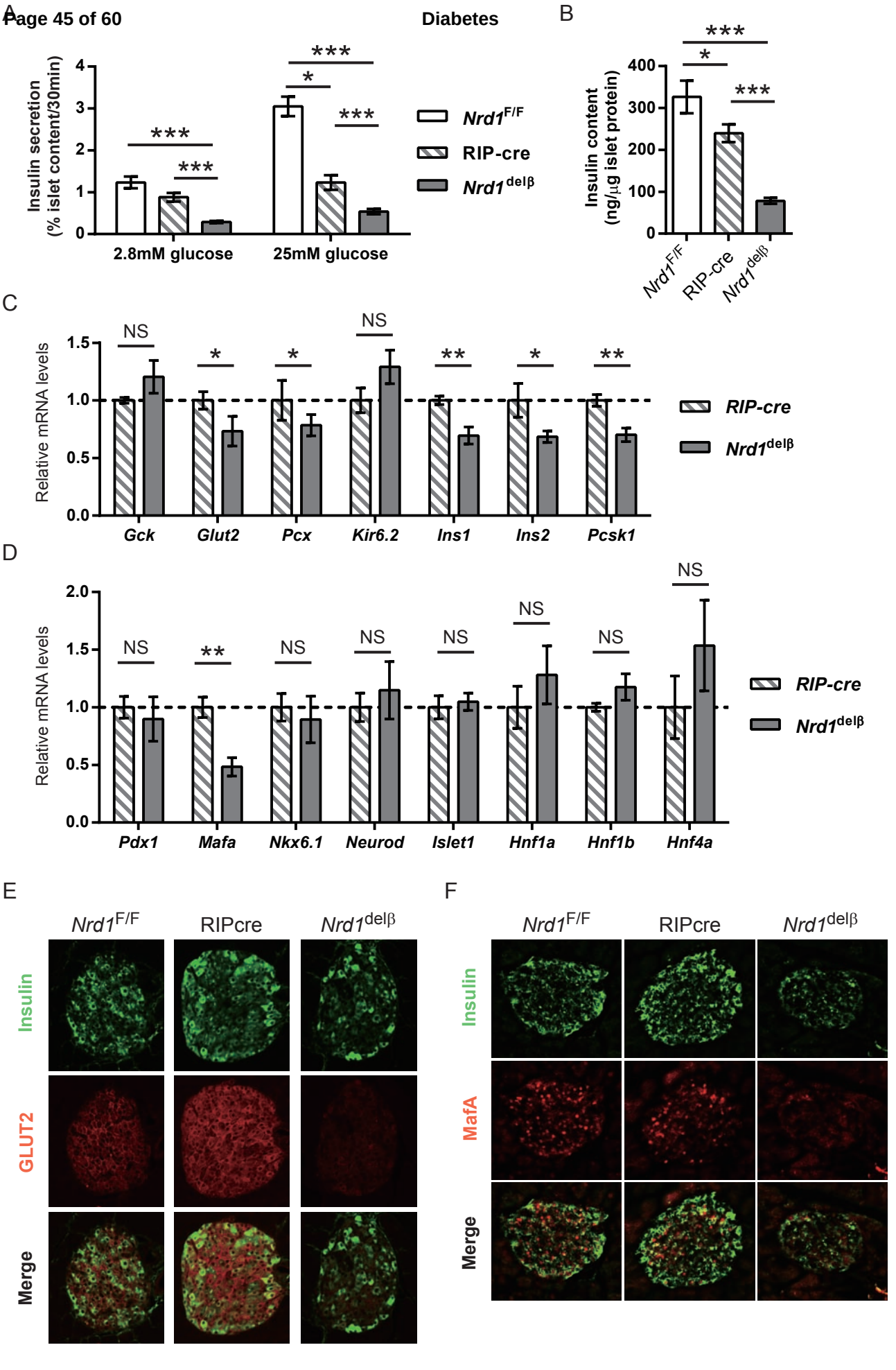
A
Insulin secretion (% islet content/30min)
2.8mM glucose
25mM glucose
Nrd1F/F
RIP-cre
Nrd1delβ
B
Insulin content (ng/μg islet protein)
C
Relative mRNA levels
Gck
Glut2
Pcx
Kir6.2
Ins1
Ins2
Pcsk1
D
Pdx1
Mafa
Nkx6.1
Neurod
Islet1
Hnf1a
Hnf1b
Hnf4a
E
F
Insulin
GLUT2
MafA
Merge
RIPcre

Figure 3

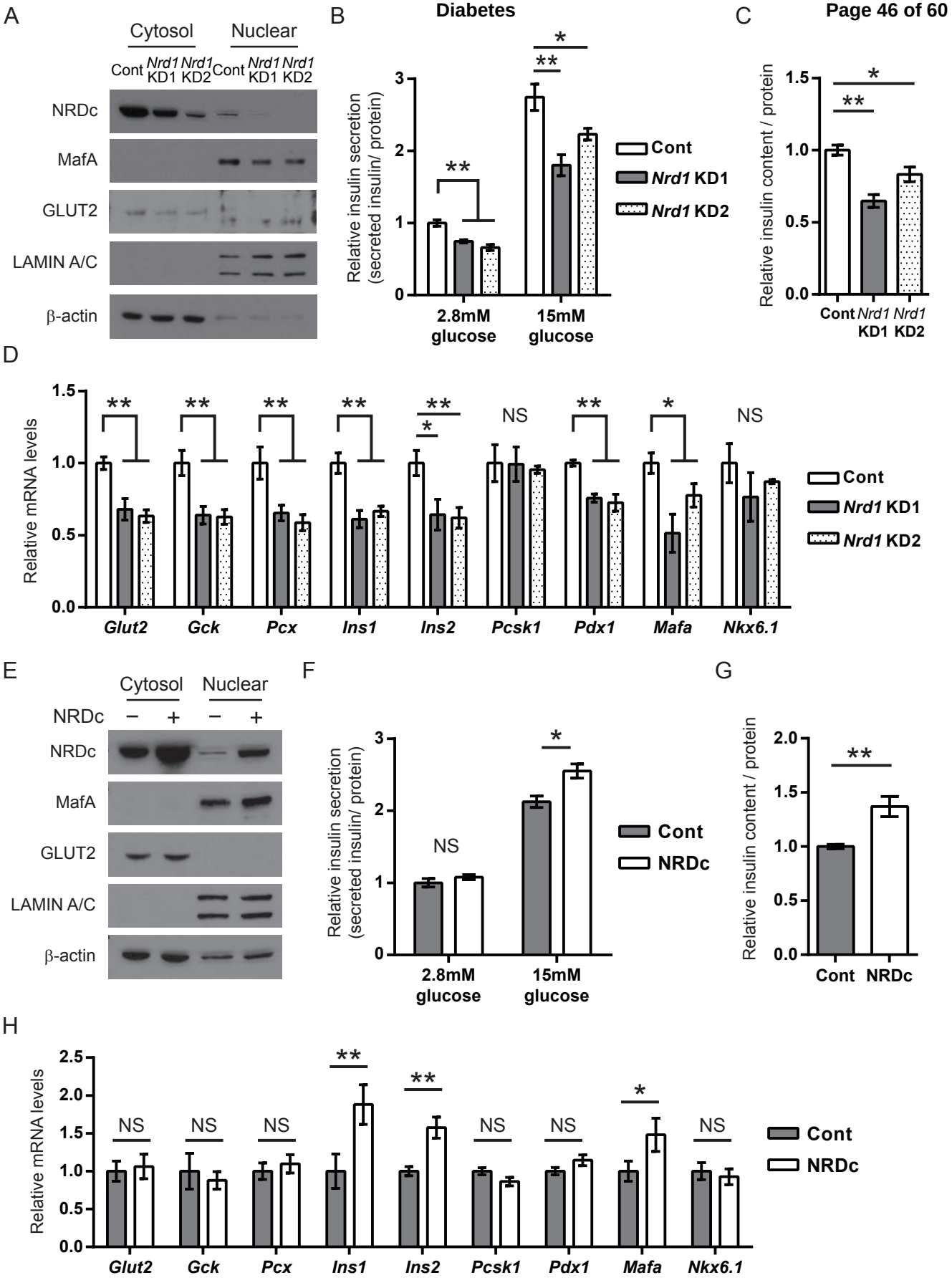
A
Cytosol
Nuclear
Cont
Nrd1 KD1
Nrd1 KD2
Cont
Nrd1 KD1
Nrd1 KD2
NRDc
MafA
GLUT2
LAMIN A/C
β-actin
B
Relative insulin secretion (secreted insulin/ protein)
2.8mM glucose
15mM glucose
Cont
Nrd1 KD1
Nrd1 KD2
C
Relative insulin content / protein
Cont
Nrd1 KD1
Nrd1 KD2
D
Relative mRNA levels
Glut2
Gck
Pcx
Ins1
Ins2
Pcsk1
Pdx1
Mafa
Nkx6.1
NS
Cont
Nrd1 KD1
Nrd1 KD2
E
Cytosol
Nuclear
NRDc
NRDc
MafA
GLUT2
LAMIN A/C
β-actin
F
Relative insulin secretion (secreted insulin/ protein)
NS
2.8mM glucose
15mM glucose
Cont
NRDc
G
Relative insulin content / protein
Cont
NRDc
H
Relative mRNA levels
NS
Glut2
Gck
Pcx
Ins1
Ins2
Pcsk1
Pdx1
Mafa
Nkx6.1
Cont
NRDc

Figure 4

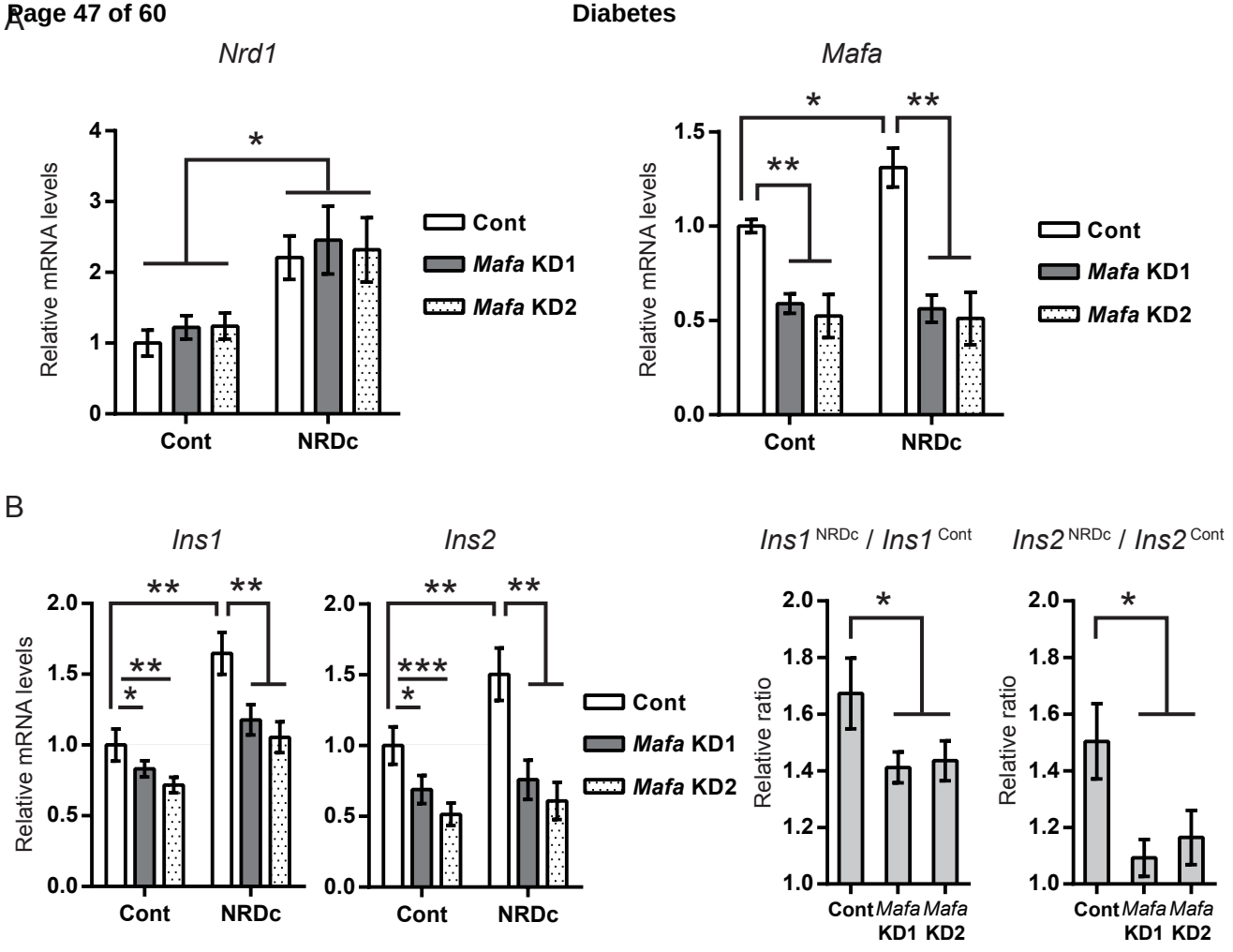
A
Nrd1
Relative mRNA levels
Cont
NRDc
Cont
Mafa KD1
Mafa KD2
Mafa
B
Ins1
Ins2
Ins1 NRDc / Ins1 Cont
Ins2 NRDc / Ins2 Cont
Relative ratio
Cont
Mafa KD1
Mafa KD2

Figure 5

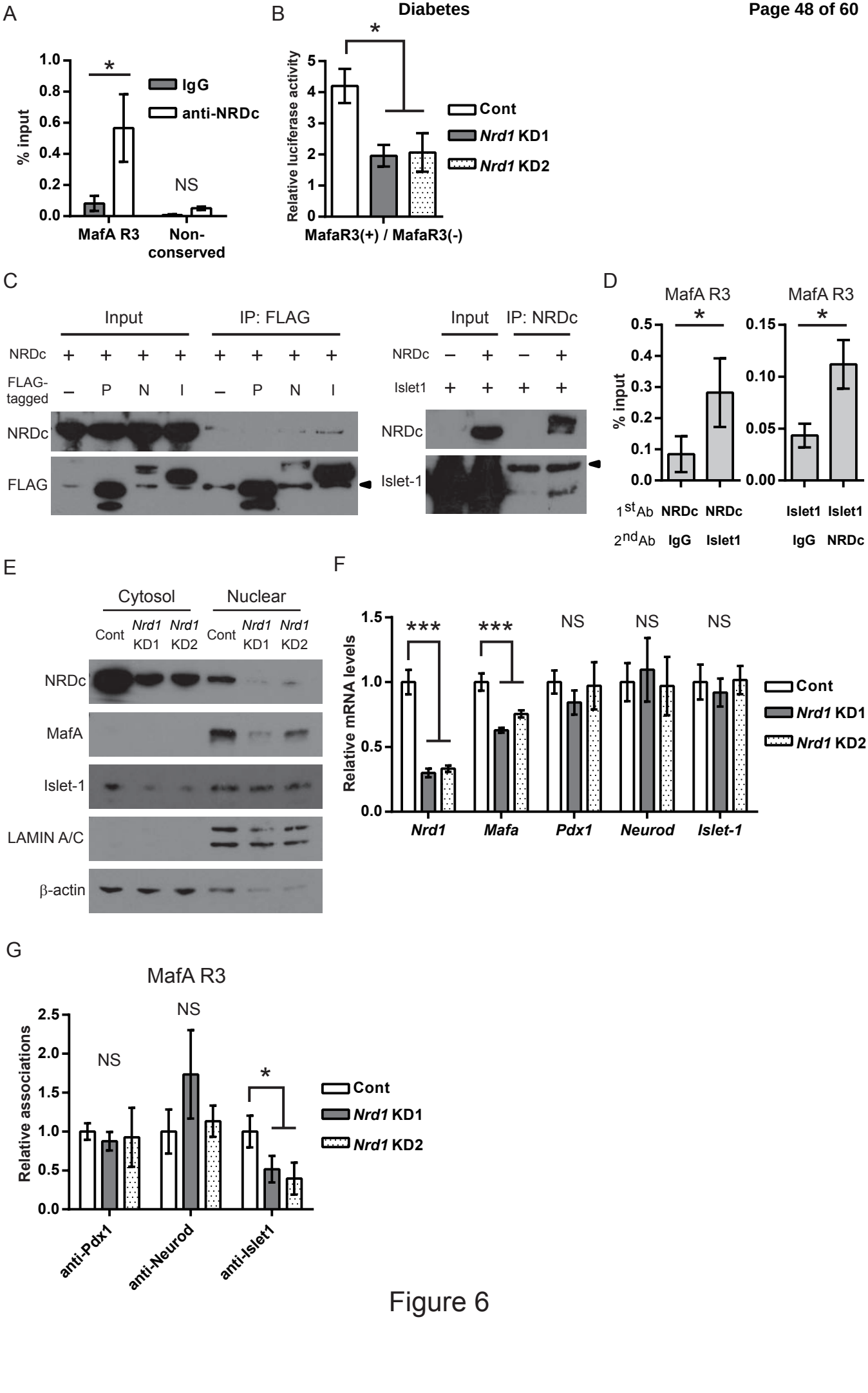
A
% input
IgG
anti-NRDc
NS
MafA R3
Non-conserved
B
Relative luciferase activity
Cont
Nrd1 KD1
Nrd1 KD2
MafaR3(+) / MafaR3(-)
C
Input
IP: FLAG
Input
IP: NRDc
NRDc
FLAG-tagged
Islet1
FLAG
Islet-1
D
MafA R3
MafA R3
% input
1st Ab
2nd Ab
NRDc
IgG
Islet1
E
Cytosol
Nuclear
Cont
Nrd1 KD1
Nrd1 KD2
NRDc
MafA
Islet-1
LAMIN A/C
β-actin
F
Relative mRNA levels
Nrd1
Mafa
Pdx1
Neurod
Islet-1
G
MafA R3
Relative associations
anti-Pdx1
anti-Neurod
anti-Islet1

Figure 6

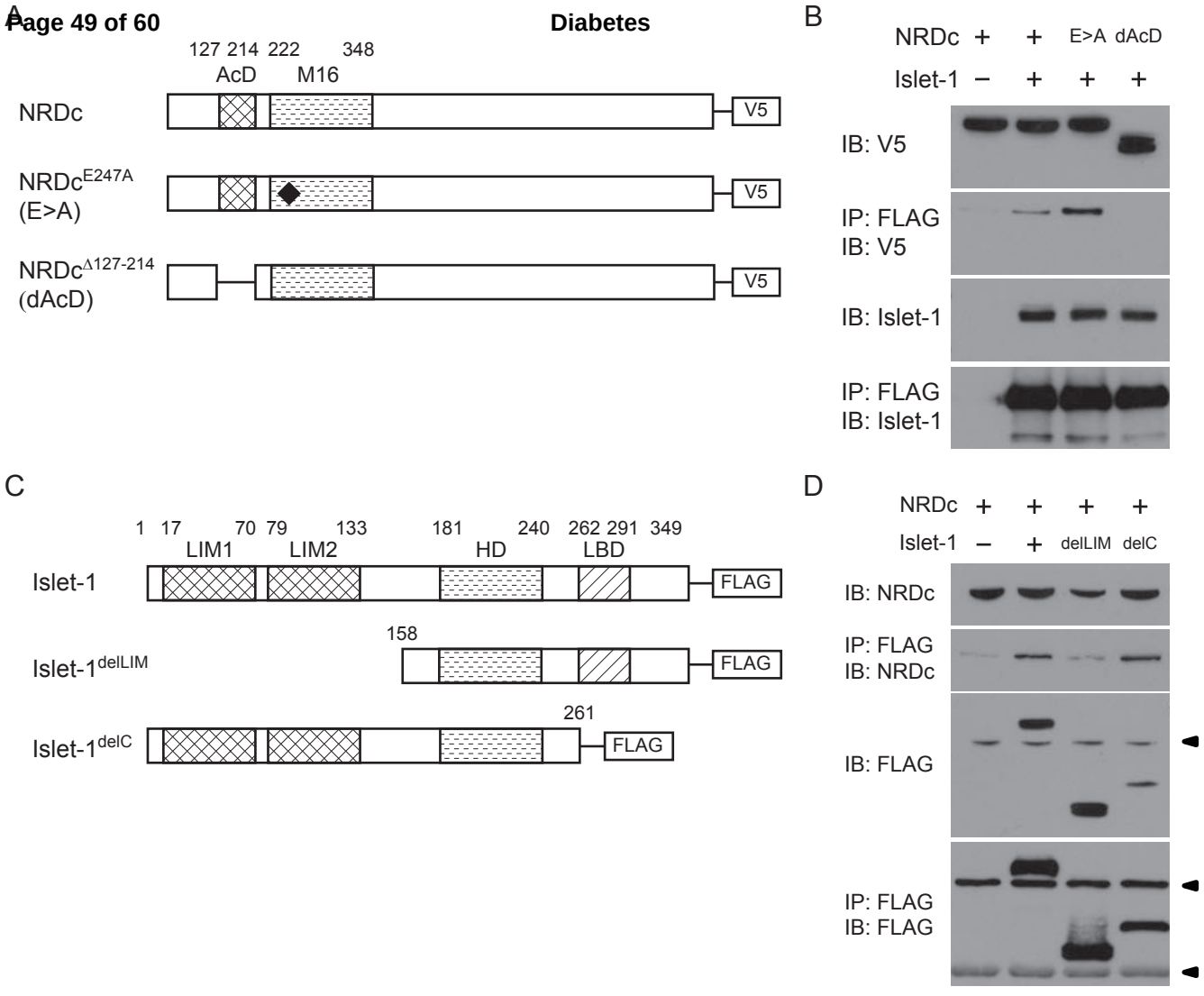
A
127 214 222 348
AcD M16
NRDc
V5
NRDc^E247A (E>A)
V5
NRDc^Δ127-214 (dAcD)
V5
B
NRDc + + E>A dAcD
Islet-1 − + + +
IB: V5
IP: FLAG IB: V5
IB: Islet-1
IP: FLAG IB: Islet-1
C
1 17 70 79 133 181 240 262 291 349
LIM1 LIM2 HD LBD
Islet-1
FLAG
158
Islet-1^delLIM
FLAG
261
Islet-1^delC
FLAG
D
NRDc + + + +
Islet-1 − + delLIM delC
IB: NRDc
IP: FLAG IB: NRDc
IB: FLAG
IP: FLAG IB: FLAG

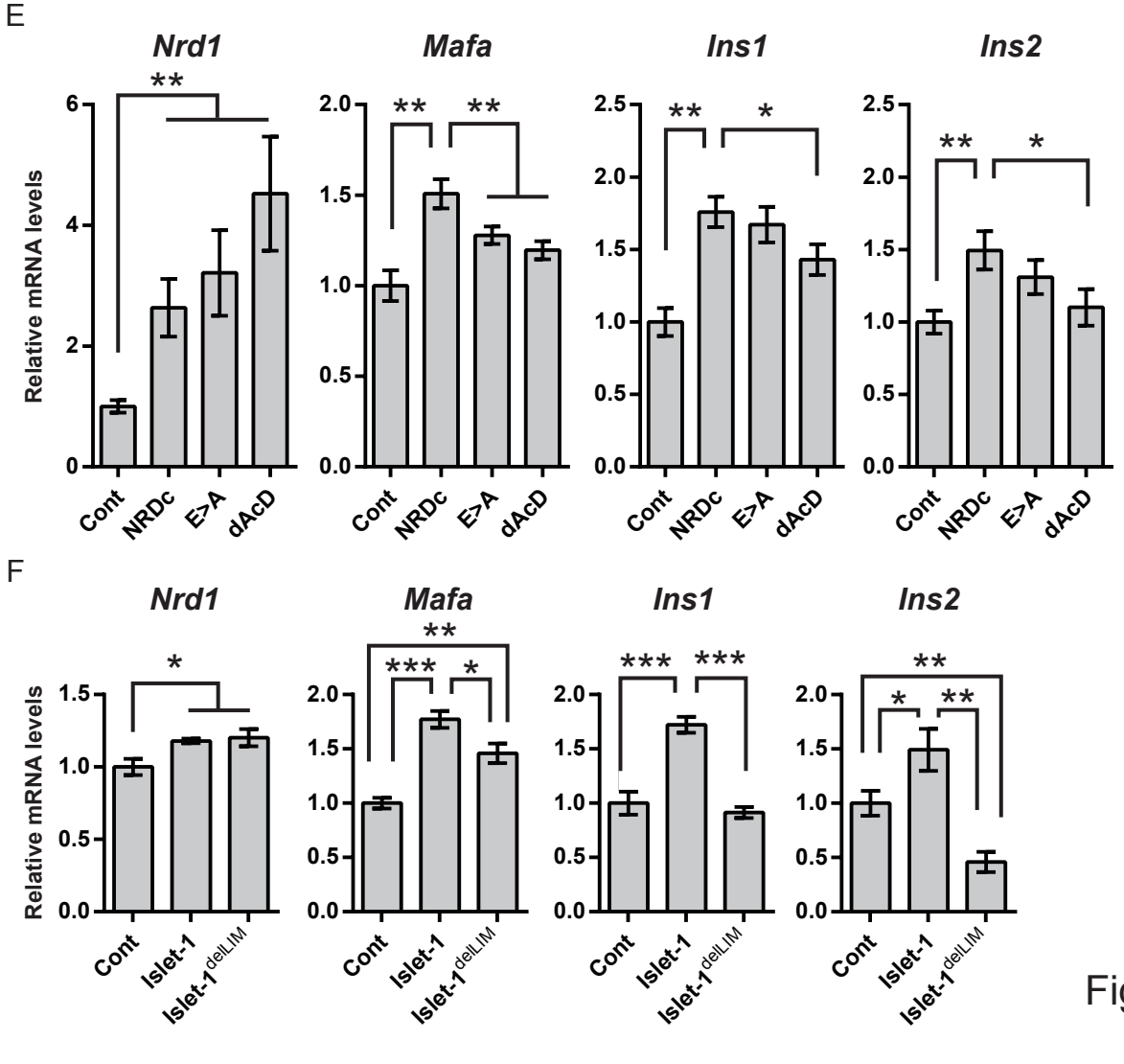
E
Nrd1
Mafa
Ins1
Ins2
Relative mRNA levels
Cont
NRDc
E>A
dAcD
F
Nrd1
Mafa
Ins1
Ins2
Relative mRNA levels
Cont
Islet-1
Islet-1^delLIM

Figure 7

Supplemental Information

Nardilysin is Required for maintaining Pancreatic β-Cell Function

Kiyoto Nishi, Yuichi Sato, Mikiko Ohno, Yoshinori Hiraoka, Sayaka Saijo, Jiro Sakamoto, Po-Min Chen, Yusuke Morita, Kanako Iwasaki, Kazu Sugizaki, Norio Harada, Yoshiko Mukumoto, Hiroshi Kiyonari, Kenichiro Furuyama, Shintaro Matsuda, Yoshiya Kawaguchi, Shinji Uemoto, Toru Kita, Nobuya Inagaki, Takeshi Kimura and Eiichiro Nishi

SUPPLEMENTAL INFORMATION INVENTORY

Supplementary Figures 1-5

Supplementary Table 1

Supplemental Experimental Procedures

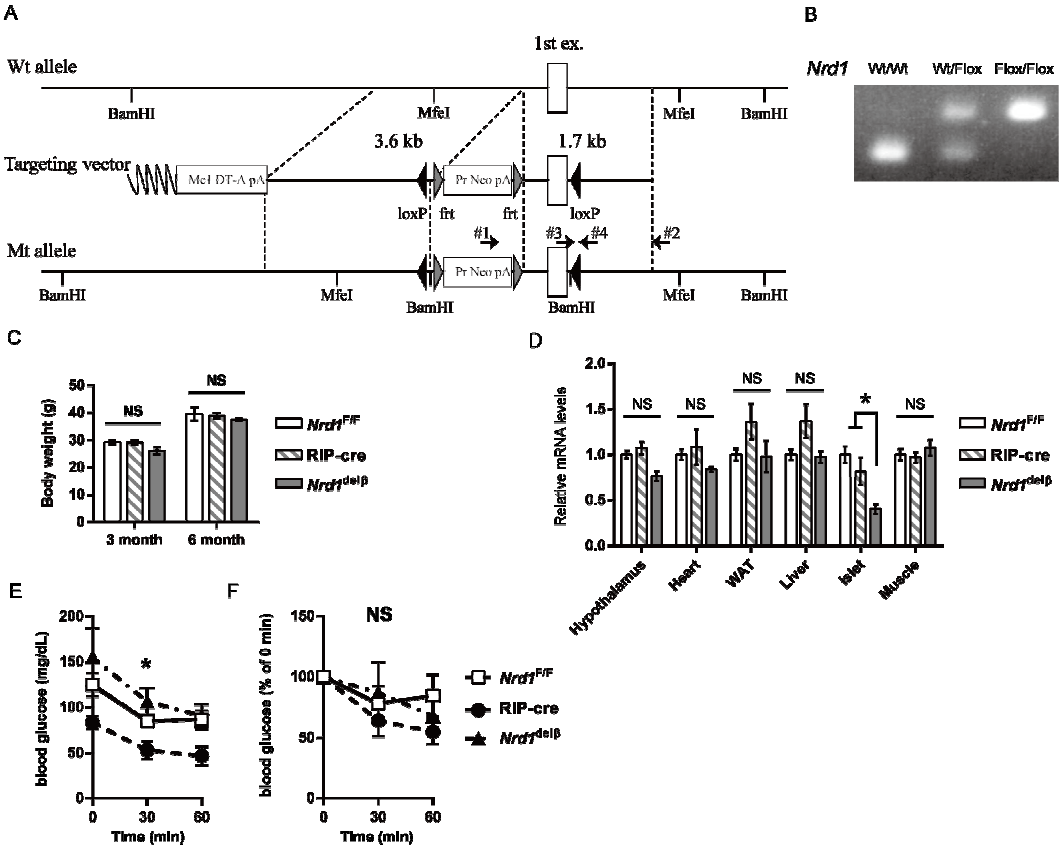

Supplementary Figure 1. (A) Structure of a part of *Nrd1*, a gene that encodes NRDc (top), the targeting vector (middle) and the mutated allele (bottom). The targeting vector was designed to insert loxP sites upstream and downstream of exon 1 of *Nrd1*. #1 (GTACTCGGATGGAAGCCGGTCTTGTC) and #2 (TCATTCAGGCAGGGTTTGAGTCACC) were the primers used for screening of the targeted ES cells. #3 (GCGATCCCAAGCAGTACCGGTG) and #4 (AAATTGCCCTGGCCGCCTCAC) were the primers used for routine genotyping of the mutant mice. (B) PCR genotyping of the *Nrd1*-floxed mice. The amplicon size is 174 bp for the wild-type allele and 234 bp for the floxed allele. (C) Body weight is similar between *Nrd1*^{delβ} and control mice (n=7-11 per genotype). (D) Relative mRNA levels of *Nrd1* in the indicated organs from 6-month-old *Nrd1*^{delβ} and control mice (n=4-5 per genotype). WAT: epididymal fat, Muscle: quadriceps femoris muscle. (E, F) Insulin tolerance test (i.p. injection of 2 U/kg insulin) reveals unaltered insulin sensitivity in 6-month-old *Nrd1*^{delβ} mice (n=5-6 per genotype). * $p<0.05$ for *Nrd1*^{delβ} vs. Rip-cre, NS: not significant

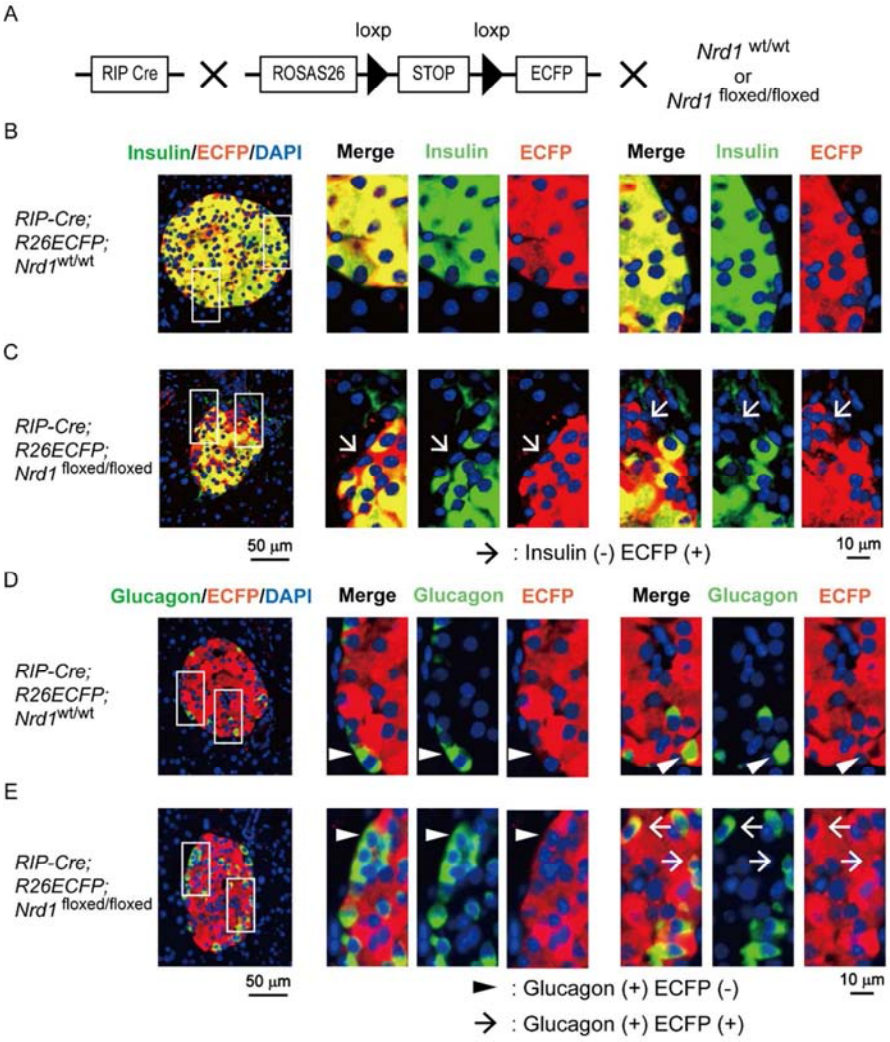

Supplementary Figure 2. (A) *Nrd1*$^{flox/flox}$ mice were crossed with RIPCre and R26ECFP mice to generate RIPCre;R26ECFP;*Nrd1*$^{flox/flox}$ and RIPCre;R26ECFP;*Nrd1*$^{wt/wt}$ mice. (B, C) Pancreata from 6- to 8-month-old RIPCre;R26ECFP;*Nrd1*$^{wt/wt}$ and RIPCre;R26ECFP;*Nrd1*$^{flox/flox}$ mice was stained with anti-insulin (green) and anti-ECFP (red) antibodies. The Arrow indicates insulin (-), ECFP (+) cell. (D, E) Pancreata from the mice described in (B, C) was stained with anti-glucagon (green) and anti-ECFP (red) antibodies. The Arrowhead and Arrow indicate glucagon (+), ECFP (-) and glucagon (+), ECFP (+) cells, respectively.

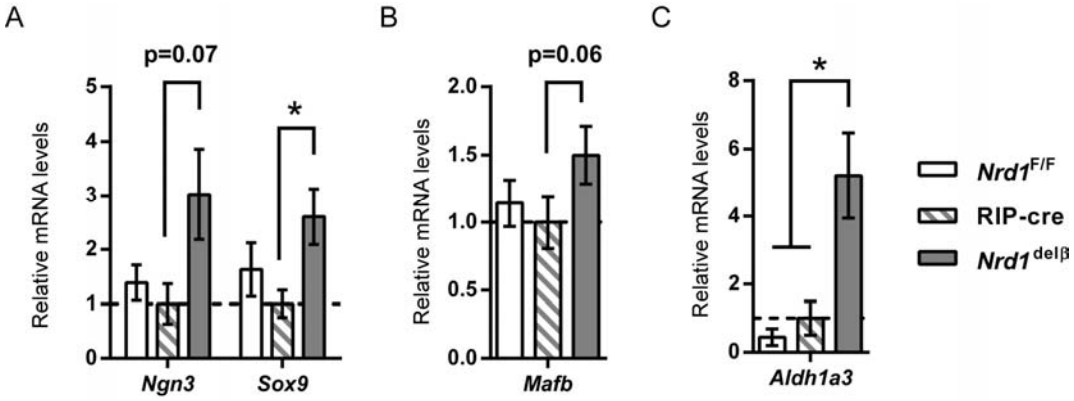

Supplementary Figure 3. Relative mRNA levels of *Ngn3, Sox9* (A), *Mafb* (B) and *Aldh1a3* (C) in isolated islets from 6- to 8-month-old *Nrd1*$^{del\beta}$ and control mice. Levels of RIP-cre control mice were normalized to 1 (n=4-5 per genotype). * $p<0.05$.

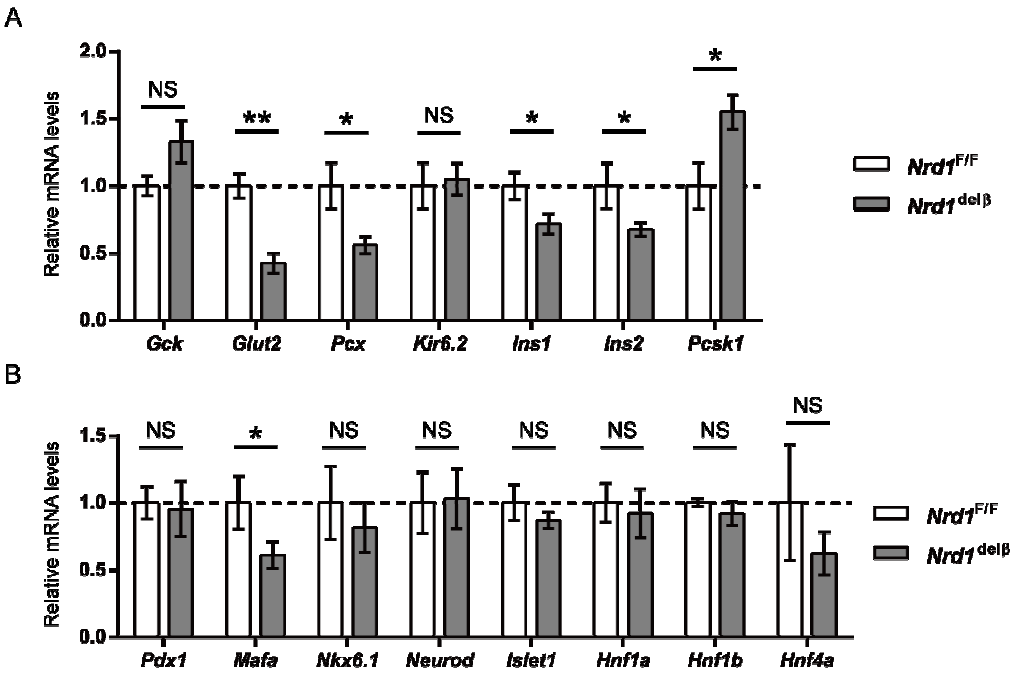

Supplementary Figure 4. Relative mRNA levels of genes involved in insulin secretion (A) and transcriptional factors (B) in isolated islets from 6- to 8-month-old *Nrd1*$^{del\beta}$ and *Nrd1*$^{flox/flox}$ mice, as measured by qRT-PCR. Levels of *Nrd1*$^{flox/flox}$ control mice were normalized to 1 (n=4-5 per genotype). * $p<0.05$, ** $p<0.01$.

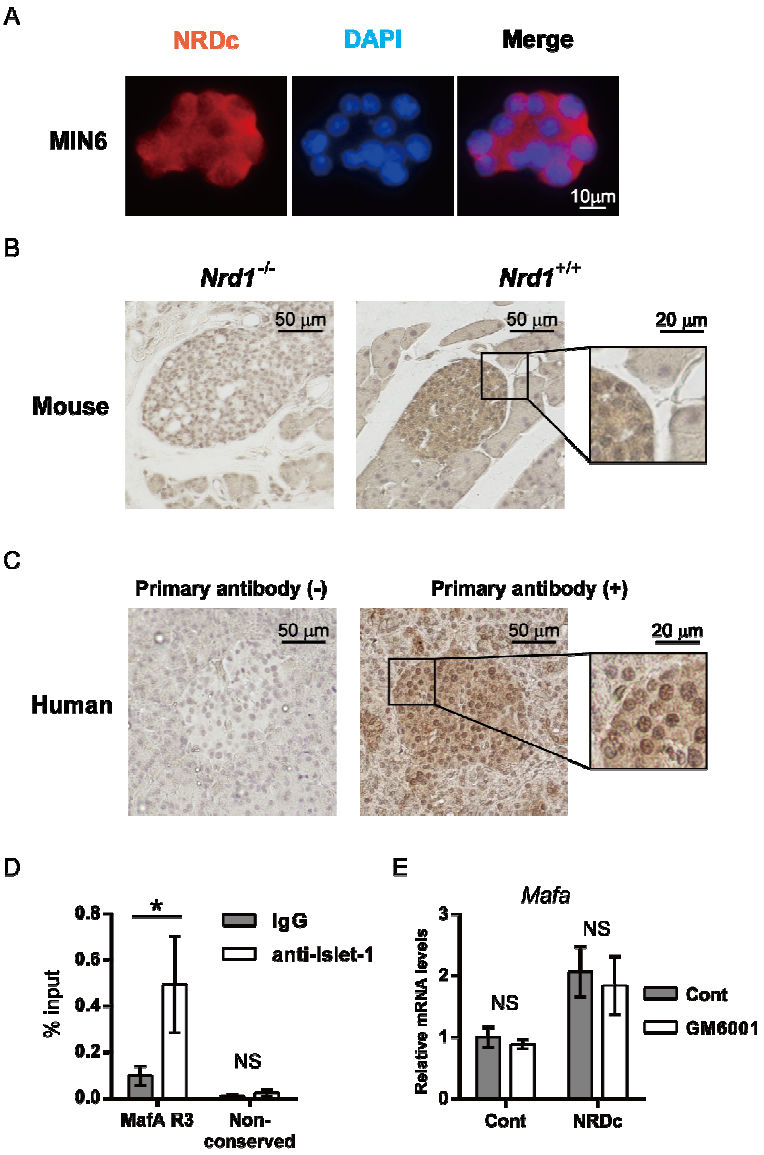

Supplementary Figure 5. (A) MIN6 cells were stained with anti-mouse NRDc antibody (red) and counterstained with DAPI (blue). (B, C) Pancreata from 3-month-old wild-type mice (B) and human (C) were stained with anti-mouse and human NRDc antibody, respectively, and counterstained with hematoxylin. (D) ChIP with anti- Islet-1 antibody followed by qRT-PCR demonstrates that Islet-1binds to the enhancer region of MafA. Results were normalized to input DNA (n = 6). MafA R3: -8118 to -7750 relative to the transcriptional start site (TSS) of *Mafa*; Non-conserved: -1678 to -1560 relative to the TSS of *Mafa.* (E) Relative mRNA levels of *Mafa* in control or NRDc-overexpressing INS 832/13 cells. Cells were treated for 24 hours with or without

GM6001 (25μM) (n=5).

Supplementary Table 1. List of primers used in qRT-PCR.

Gene	Forward	Reverse
M,R Nrd1	ATGGATGGCCTTTCCCTTG	CGCGAAGTTCAGCTTGTCAA
M Gck	TGTACAAGCTGCACCCGAGCTTCA	TGGATTTCACTGGCCCAGCATGCAA
M Glut2	CATTCTTTGGTGGGTGGC	CCTGAGTGTGTTTGGAGCG
M Pcx	GATGACCTCACAGCCAAGCA	GGGTACCTCTGTGTCCAAAGGA
M Kir6.2	AGGGGTCCTGTGCTTGCCATACAA	AGACAAAGTGACTCACAGCTGCCCA
M Ins1	GAAGCGTGGCATTGTGGAT	TGGGCCTTAGTTGCAGTAGTTCT
M Ins2	AGCCCTAAGTGATCCGCTACAA	CATGTTGAAACAATAACCTGGAAGA
M Pcsk1	GACCTGCACAATGACTGCAC	GGTCCAGACAACCAGATGCT
M Pdx1	CATCTCCCCATACGAAGTGC	GGGGCCGGGAGATGTATTTG
M Mafa	TTCAGCAAGGAGGAGGTCAT	CCGCCAACTTCTCGTATTTC
M NKx6.1	GAGTGATGCAGAGTCCGCCGT	GCTGTCCAGAGAACGTGGGTCTG
M Neurod	ATTCGCCCACGCAGAAGGCA	GACCTTGGGGCTGAGGCTCG
M Hnf1a	GTGGCGAAGATGGTCAAGTC	GCGTGGGTGAATTGCTGAG
M Hnf1b	GCCTGAACCAATCCCACCTC	TGACTGCTTTTGTCTGTCATGT
M Hnf4a	TAACACGATGCCCTCTCACCT	GGCAGGAGCTTGTAGGATTCA
M tIslet-1	CGGAGAGACATGATGGTGGTT	GGGCTGATCTATGTCGCTTTGC
M Sox9	GTACCCGCATCTGCACAACG	GATTGCCCAGAGTGCTCGC
M Gapdh	CCAGAACATCATCCCTGCATC	CCTGCTTCACCACCTTCTTGA
M β-actin	CTGACTGACTACCTCATGAAGATCCT	CTTAATGTCACGCACGATTTCC
R Glut2	TCAGCCAGCCTGTGTATGCA	TCCACAAGCAGCACAGAGACA
R Gck	AGTATGACCGGATGGTGGAT	CCGTGGAACAGAAGGTTCTC
R Pcx	TTGAAGGATGTGAAGGGCC	ACCTTTCGGATAGTGCCCTC
R Ins1	ACCTTTGTGGTCCTCACCTG	AGCTCCAGTTGTGGCACTTG
R Pcsk1	CAGGGGAGACAAGGAAAAG	AGGCACTGCTGATAGAGATGG
R Pdx1	GGATGAAATCCACCAAAGCTC	TTCCACTTCATGCGACGGT
R Mafa	CGAGTACGTCAACGACTTCG	AAGAGGGCACCGAGGAGCAG
R Nkx6.1	TCTTCTGGCCTGGGGTGATG	GGCTGCGTGCTTCTTTCTCCA
R β-actin	GATTACTGCCCTGGCTCCTA	TCATCGTACTCCTGCTTGCT
ChIP MafA R3 (-8118 to -7750)	CACTCAGCCTTGTTTAGGAGAGAAAAGA	CCGAGCTGCGTGGGGTTTAT
ChIP MafA Non-conserved (-1678 to -1560)	CCAGTTGCTTTTCACGGCCTC	CGGGGAGCCATTGGAATGTC

M = mouse; R = rat

Supplemental Experimental Procedures

Plasmids

cDNAs encoding the full lengths of mouse PDX-1, Islet-1 and NeuroD were cloned into pME18s-FLAG. Deletion mutants of Islet-1, pME18s- Islet-1 $_{1\text{-}261}$ and pME18s- Islet-1 $_{158\text{-}349}$, were generated by PCR. pcDNA3.1-mNRDc-V5 was constructed as described previously (Nishi et al., 2006). Transfections were carried out using polyethylenimine (Polysciences) according to the manufacturer's instructions.

Antibodies and immunoblot analysis

Rat anti-mouse NRDc monoclonal antibodies (clone #1 and #135) were raised against recombinant mouse NRDc in our laboratory (Hiraoka et al., 2014). Mouse anti-human NRDc monoclonal antibody (#102) was raised against the GST fusion protein containing the N-terminal fragment (M^{50} to D^{129}) of human NRDc in our laboratory. For the production of mouse anti-mouse NRDc monoclonal antibody (2E6), *Nrd1*$^{-/-}$ mice were immunized with the C-terminal fragment of mouse NRDc (G^{348} to K^{1161}), which was synthesized by using silkworm protein expression system (Sysmex). Other antibodies were from the following sources: lamin A/C (Santa Cruz), β-actin (Santa Cruz), FLAG (Sigma), Islet-1 (Abcam), Glut2 (Santa Cruz), NeuroD (Santa Cruz), Pdx1 (Santa Cruz) and MafA (Bethyl).

Preparations of total cell extract and the immunoblot experiment were carried out as described previously (Hiraoka et al., 2014). In brief, cells were lysed in buffer

containing 10 mM Tris–HCl pH 7.4, 150 mM NaCl, 1% NP-40, protease inhibitor cocktail (Roche) and phosphatase inhibitor cocktail (Sigma). Cell lysates were separated by SDS–polyacrylamide gel electrophoresis and transferred to nitrocellulose filters. After blocking, filters were incubated with primary antibodies, followed by horseradish-peroxidase-conjugated secondary antibodies. The immobilized peroxidase activity was detected with an enhanced chemiluminescence system (Millipore). For the isolation of nuclei, cells were suspended in hypotonic buffer containing 10 mM HEPES (pH 7.9), 1.5 mM MgCl2, 10 mM KCl, 0.1 mM EDTA, 0.1% NP-40, 1 mM dithiothreitol, protease inhibitor cocktail (Roche) and phosphatase inhibitor cocktail (Sigma), followed by homogenization and centrifugation (3000 r.p.m., 5 min). Isolated nuclei were then resuspended in high-salt buffer containing 20 mM HEPES (pH 7.9), 1.5 mM MgCl2, 400 mM NaCl, 0.1 mM EDTA, 10% glycerol, 0.1% NP-40, 1 mM dithiothreitol, protease inhibitor cocktail (Roche) and phosphatase inhibitor cocktail (Sigma), followed by centrifugation (13,200 r.p.m., 5 min).

Immunostaining and Histological analysis

Immunocytochemistry was performed as described previously (Nishi et al., 2006). Briefly, fixed MIN6 cells were incubated with rat monoclonal anti-mouse NRDc antibody (clone #135), followed by incubation with the secondary antibody (Alexa Fluor 488-conjugated goat antibody to mouse IgG) and counterstaining with DAPI. Immunohistochemistry was performed as described previously (Ohno et al., 2014; Ohno et al., 2009). For mouse islet, we used anti-mouse monoclonal NRDc antibody (clone

#135), guinea pig antibody to insulin (Dako, 1:800), rabbit antibody to glucagon (Dako, 1:400) and rabbit antibody to MafA (Abcam, 1:500). After incubation with the primary antibodies, the sections were washed in PBS and incubated with secondary antibodies, Cy3-conjugated donkey antibody to guinea pig IgG (Millipore, 1:500) and Alexa Fluor 488-conjugated donkey antibody to rabbit IgG (Invitrogen, 1:200), for 1 h, followed by counterstaining with DAPI. For lineage tracing study, pancreatic sections from *Nrd1*$^{floxed/floxed}$; RIP-Cre; R26ECFP and *Nrd1*$^{wt/wt}$; RIP-Cre; R26ECFP mice were compared. Mouse antibody to glucagon (Santa Cruz, 1:800) and rabbit antibody to ECFP (Sigma, 1:100) were used as primary antibodies.

Pictures of immunostained sections were acquired using a BZ-9000 digital microscope (Keyence) and analyzed with dedicated software (Dynamic Cell Count System, BZ-HIC). For the estimation of β-cell mass, four pancreatic tissue sections (at least 50 μm apart each other) were analyzed in each mouse. Pictures of the whole pancreas were obtained by combining 48-108 pictures at magnification x4 in each section using the image stitching function of BZ-9000. The ratio of insulin-positive area to pancreatic area was calculated in each section, and the proportions of four sections were averaged and multiplied by the pancreatic weight of each mouse. The ratio of α-cell area to α- and β-cell area was estimated by the calculation of the proportion of glucagon-positive area to insulin- and glucagon-positive area, which was calculated by using pictures at magnification x10 acquired from the same section used for the estimation of the β-cell mass.

For the immunostaining of human pancreata, non-cancerous regions from

surgically resected specimens were obtained from patients with pancreatic cancer or neuroendocrine tumor admitted to Kyoto University Hospital. Written informed consent for the use of resected tissue samples was obtained from all patients in accordance with the Declaration of Helsinki, and the study was approved by Ethical Committee on Human Research of Kyoto University Graduate School of Medicine. For the primary antibody, we used mouse monoclonal anti-human NRDc antibody (clone #102).

Quantitative real-time PCR (qRT-PCR) analysis

Total RNA was purified from freshly isolated islets, MIN6 cells and INS 832/13 cells using Trizol reagent (Invitrogen) according to the manufacturer's protocol. First-strand cDNA was synthesized from total RNA using the Transcriptor First Strand cDNA Synthesis Kit (Roche). qRT-PCR was carried out using the LightCycler 96 system (Roche) and THUNDERBIRD SYBR qPCR (TOYOBO, Japan) following the manufacturers' directions. The results were standardized for comparison by measuring the level of Gapdh or Actb mRNA in each sample. The primers used are listed in Table S2.